

Calorimetry

concept & examples

Programme

Lesson 1

Why build calorimeters ?
Electromagnetic showers
Detection processes

Lesson 2

Recap
EM calorimeters
Hadronic showers
Jets & Missing Transverse Energy
CMS & ATLAS calorimeters

Lesson 3

Other calorimeters
Calorimeter R&Ds for future
colliders

Tutorial

Detecting EM showers - $H \rightarrow \gamma\gamma$
A few numbers

RECAP: ELECTROMAGNETIC SHOWERS

The shower develops as a **cascade** by **energy transfer** from the incident particle to a **multitude of particles** (e^\pm and γ).

The **number of cascade particles** is **proportional** to the **energy deposited** by the incident particle.

The role of the calorimeter is to **count** these cascade particles.

The relative occurrence of the various processes is a function of the material (Z)

The radiation length (X_0) allows to universally describe the shower development

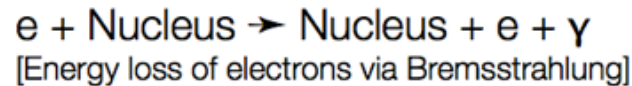
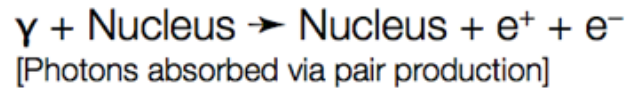
A SIMPLE EM SHOWER MODEL

Simple shower model:

[from Heitler]

Only two dominant interactions:

Pair production and Bremsstrahlung ...



Shower development governed by X_0 ...

After a distance X_0 electrons remain with only $(1/e)^{\text{th}}$ of their primary energy ...

Photon produces e^+e^- -pair after $9/7X_0 \approx X_0$...

Assume:

$E > E_c$: no energy loss by ionization/excitation

$E < E_c$: energy loss only via ionization/excitation



Use
Simplification:

$$E_\gamma = E_e \approx E_0/2$$

[E_e loses half the energy]

$$E_e \approx E_0/2$$

[Energy shared by e^+/e^-]

... with initial particle energy E_0

A SIMPLE EM SHOWER MODEL

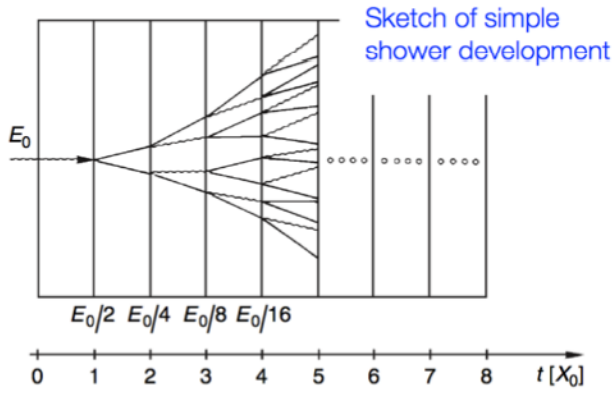
Simple shower model: [continued]

Shower characterized by:

- Number of particles in shower
- Location of shower maximum
- Longitudinal shower distribution
- Transverse shower distribution

Longitudinal components;
measured in radiation length ...

... use: $t = \frac{x}{X_0}$



Number of shower particles
after depth t:

$$N(t) = 2^t$$

Energy per particle
after depth t:

$$E = \frac{E_0}{N(t)} = E_0 \cdot 2^{-t}$$

→ $t = \log_2(E_0/E)$

Total number of shower particles
with energy E_1 :

$$N(E_0, E_1) = 2^{t_1} = 2^{\log_2(E_0/E_1)} = \frac{E_0}{E_1}$$

Number of shower particles
at shower maximum:

$$N(E_0, E_c) = N_{\max} = 2^{t_{\max}} = \frac{E_0}{E_c}$$

Shower maximum at:

$$t_{\max} \propto \ln(E_0/E_c)$$

$$\propto E_0$$

A SIMPLE EM SHOWER MODEL

Simple shower model: [continued]

Longitudinal shower distribution increases only logarithmically with the primary energy of the incident particle ...

Some numbers: $E_c \approx 10$ MeV, $E_0 = 1$ GeV $\rightarrow t_{\max} = \ln 100 \approx 4.5$; $N_{\max} = 100$
 $E_0 = 100$ GeV $\rightarrow t_{\max} = \ln 10000 \approx 9.2$; $N_{\max} = 10000$

$$t_{\max}[X_0] \sim \ln \frac{E_0}{E_c}$$

EM LONGITUDINAL DEVELOPMENT

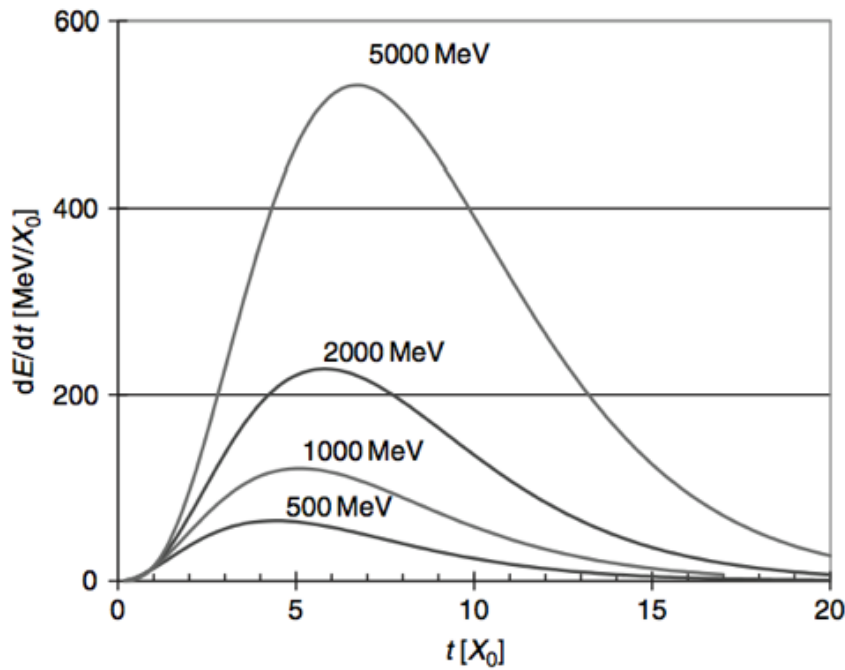
Longitudinal profile

Parametrization:
[Longo 1975]

$$\frac{dE}{dt} = E_0 t^\alpha e^{-\beta t}$$

- α, β : free parameters
- t^α : at small depth number of secondaries increases ...
- $e^{-\beta t}$: at larger depth absorption dominates ...

Numbers for $E = 2$ GeV (approximate):
 $\alpha = 2, \beta = 0.5, t_{\max} = \alpha/\beta$



More exact
[Longo 1985]

$$\frac{dE}{dt} = E_0 \cdot \beta \cdot \frac{(\beta t)^{\alpha-1} e^{-\beta t}}{\Gamma(\alpha)}$$

[Γ : Gamma function]

$$\rightarrow t_{\max} = \frac{\alpha - 1}{\beta} = \ln\left(\frac{E_0}{E_c}\right) + C_{e\gamma}$$

with:

- $C_{e\gamma} = -0.5$ [γ -induced]
- $C_{e\gamma} = -1.0$ [e-induced]

CALORIMETER ENERGY RESOLUTION

Calorimeter energy resolution determined by fluctuations ...

Homogeneous calorimeters:

- Shower fluctuations
 - Photo-electron statistics
 - Shower leakage
 - Instrumental effects (noise, light attenuation, non-uniformity)
- } Quantum fluctuations

In addition for

Sampling calorimeters:

- Sampling fluctuations
- Landau fluctuations
- Track length fluctuations

$$\frac{\sigma_E}{E} = \frac{a}{\sqrt{E}} \oplus \frac{b}{E} \oplus c$$

| | |
|---------------------------|------------------------|
| Quantum fluctuations | $\sim 1/\sqrt{E}$ |
| Electronic noise | $\sim 1/E$ |
| Shower leakage* | $\approx \text{const}$ |
| Sampling fluctuations | $\sim 1/\sqrt{E}$ |
| Landau fluctuations | $\sim 1/\sqrt{E}$ |
| Track length fluctuations | $\sim 1/\sqrt{E}$ |

* Different for longitudinal and lateral leakage ...
Complicated; small energy dependence ...

EM ENERGY RESOLUTION

Detectable signal is proportional to the number of potentially detectable particles in the shower $N_{\text{tot}} \propto E_0/E_c$

Total track length $T_0 = N_{\text{tot}} \cdot X_0 \sim E_0/E_c \cdot X_0$

The ultimate energy resolution

$$\frac{\sigma(E)}{E} \propto \frac{1}{\sqrt{T_0}} \propto \frac{1}{\sqrt{E}}$$

Detectable track length $T_r = f_s \cdot T_0$ where f_s is the fraction of N_{tot} which can be detected by the involved detection process (Cerenkov light, scintillation light, ionisation) $E_{\text{kin}} > E_{\text{th}}$

$$\frac{\sigma(E)}{E} \propto \frac{1}{\sqrt{E}} \frac{1}{\sqrt{f_s}}$$

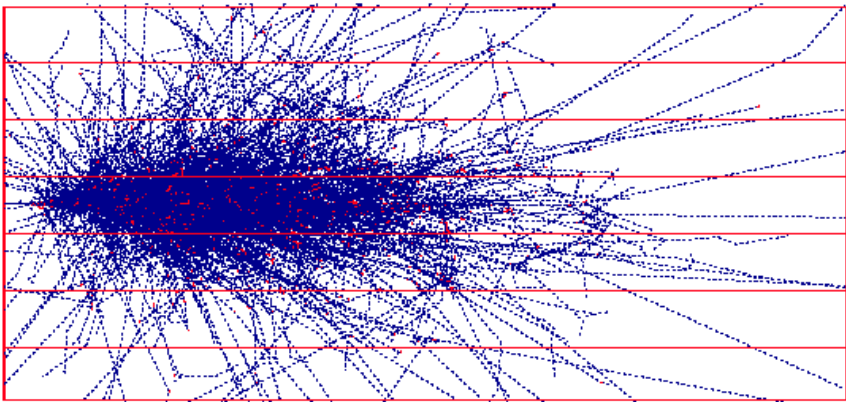
Converting back to materials ($X_0 \propto A/Z^2$, $E_c \propto 1/Z$) and fixing E

Maximise detection f_s

Minimise Z/A

$$\frac{\sigma(E)}{E} \propto \frac{1}{\sqrt{f_s}} \sqrt{\frac{E_c}{X_0}} \propto \frac{1}{\sqrt{f_s}} \sqrt{\frac{Z}{A}}$$

HOMOGENEOUS CALORIMETERS



All the energy is deposited in the active medium

Excellent energy resolution

No longitudinal segmentation

All e^\pm with $E_{kin} > E_{th}$ produce a signal

Scintillating crystals

$E_{th} \approx \beta \cdot E_{gap} \sim eV$

$\rightarrow 10^2 \div 10^4 \gamma/MeV$

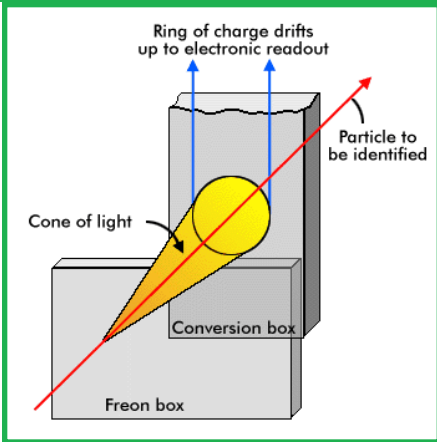
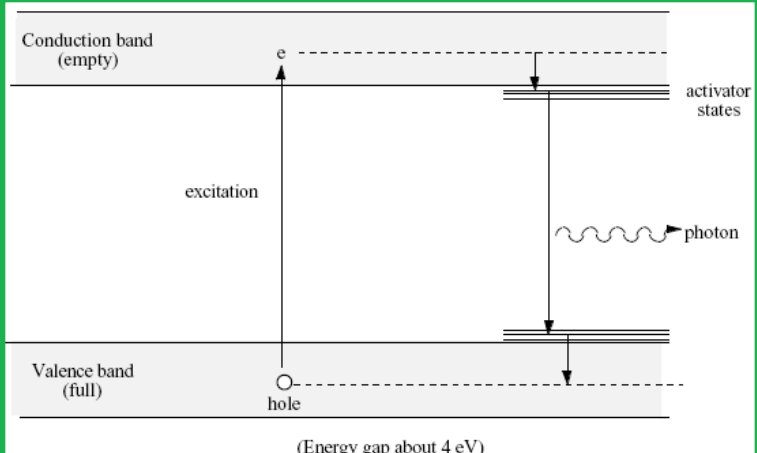
$\sigma/E \sim (1 \div 3)\% / \sqrt{E} (GeV)$

Cerenkov radiators

$\beta > 1/n \rightarrow E_{th} \approx 0.7 MeV$

$\rightarrow 10 \div 30 \gamma/MeV$

$\sigma/E \sim (5 \div 10)\% / \sqrt{E} (GeV)$



EXAMPLE

Take a Lead Glass crystal

$$E_c = 15 \text{ MeV}$$

produces Cerenkov light

Cerenkov radiation is produced par e^\pm with $\beta > 1/n$, i.e $E > 0.7\text{MeV}$

Take a 1 GeV electron

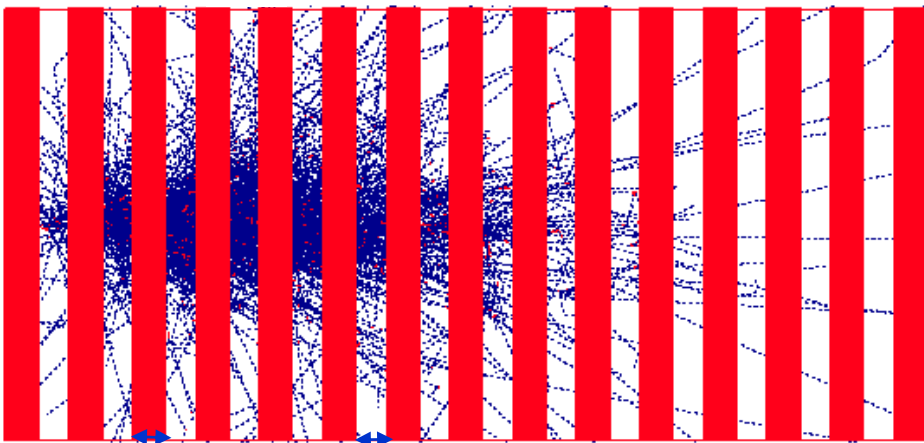
At maximum 1000 MeV/0.7 MeV e^\pm will produce light

Fluctuation $1/\sqrt{1400} = 3\%$

In addition, one has to take into account the photon detection efficiency which is typically 1000 photo-electrons/GeV: $1/\sqrt{1000} \sim 3\%$

Final resolution $\sigma/E \sim 5\%/\sqrt{E}$

SAMPLING CALORIMETERS



Shower is sampled by layers of an active medium and dense radiator

Limited energy resolution

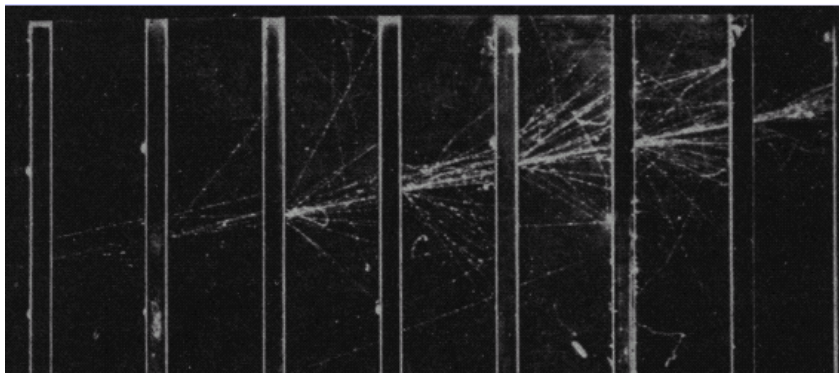
Longitudinal segmentation

Only e^\pm with $E_{\text{kin}} > E_{\text{th}}$ of the active layer produce a signal

Absorber (high Z): typically Lead, Uranium

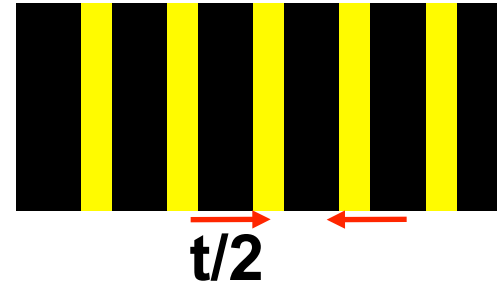
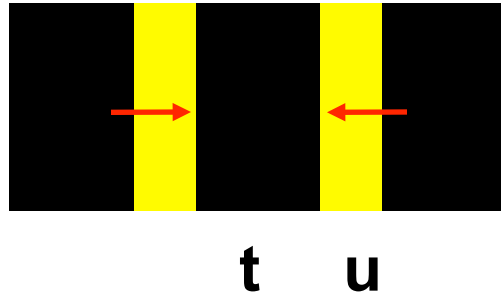
Active medium (low Z): typically Scintillators, Liquid Argon, Wire chamber

Energy resolution of sampling calorimeter dominated by fluctuations in energy deposited in the active layers



$$\sigma(E)/E \sim (10 \div 20)\% / \sqrt{E} \text{ (GeV)}$$

SAMPLING CALORIMETERS



Sampling frequency is defined by the the thickness t (in units of X_0) of the passive layers: number of times a high energy electron or photon shower is sampled

The thinner the passive layer, the better

Sampling fraction is defined by the thickness of the active layer

$$f_S = u \cdot dE/dx_{\text{active}} / [u \cdot dE/dx_{\text{active}} + t \cdot dE/dx_{\text{passive}}] \quad (u, t \text{ in } \text{gcm}^{-2}, dE/dx \text{ in } \text{MeV}/\text{gcm}^{-2}).$$

for minimum ionising particles.

SAMPLING CALORIMETERS



Most of detectable particles are produced in the absorber layers

Need to enter the active material to be counted/measured

The number of crossing of a unit “cell” N_x , using the Total Track Length

$N_x = TTL/(t+u) = E/E_c(t+u) = E/\Delta E$ where ΔE is the energy lost in a unit cell $t+u$

Assuming the statistical independence of the crossings, the fluctuations on N_x represent the “sampling fluctuations” $\sigma(E)_{\text{samp}}$

$$\sigma(E)_{\text{samp}}/E = \sigma(N_x)/N_x = 1/\sqrt{N_x} = [\Delta E(\text{GeV})/E(\text{GeV})]^{1/2} = a/\sqrt{E}$$

a is called the sampling term

SAMPLING FRACTION

The actual signal produced by the calorimeter is proportional

$$E \cdot f_s = \sum u \cdot dE/dx$$

If f_s is too small, the collected signal will be affected by electronics noise.

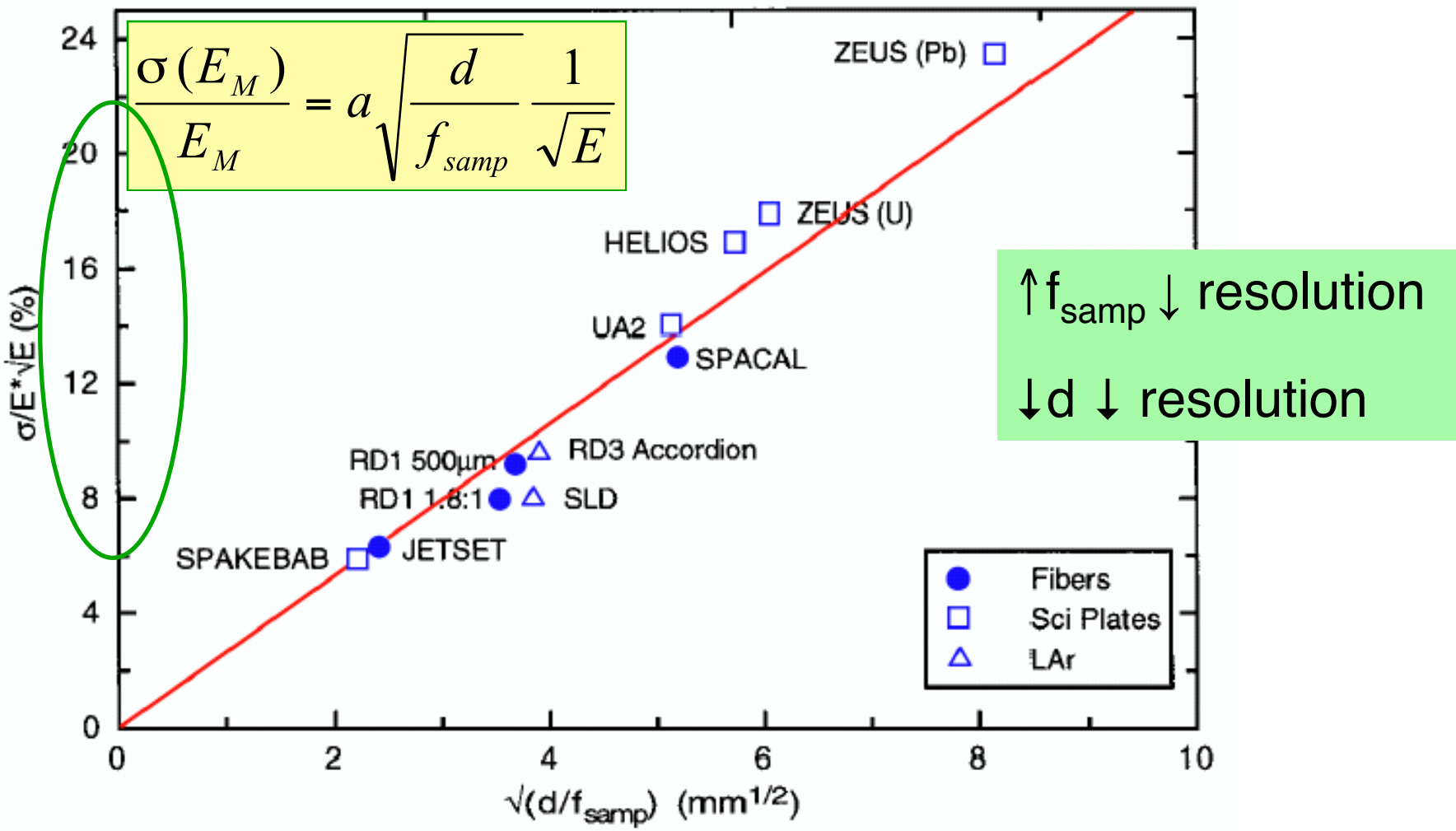
The dominant part of the calorimeter signal is not produced by minimum ionising particles (m.i.p.), but by low-energy electrons and positrons crossing the signal planes.

One defines the fractional response f_R^i of a given layer i as the ratio of energy lost in the active and of sum of active+passive layers:

$$f_R^i = E_{\text{active}}^i / (E_{\text{active}}^i + E_{\text{passive}}^i) \text{ with } \sum^i (E_{\text{active}}^i + E_{\text{passive}}^i) = E_0$$

$f_R/f_s \sim e/mip \sim 0.6$ when $Z_{\text{passive}} \gg Z_{\text{active}}$
due to transitions effects & low energy
particles not reaching the active medium

ENERGY RESOLUTION for SAMPLING CALORIMETERS



ENERGY RESOLUTION

$$\frac{\sigma}{E} = \frac{a}{\sqrt{E}} \oplus \frac{b}{E} \oplus c$$

a the **stochastic term** accounts for Poisson-like fluctuations
naturally small for homogeneous calorimeters
takes into account sampling fluctuations for sampling calorimeters

b the **noise term** (hits at low energy)
mainly the energy equivalent of the electronics noise
at LHC in particular: includes fluctuation from non primary interaction (pile-up noise)

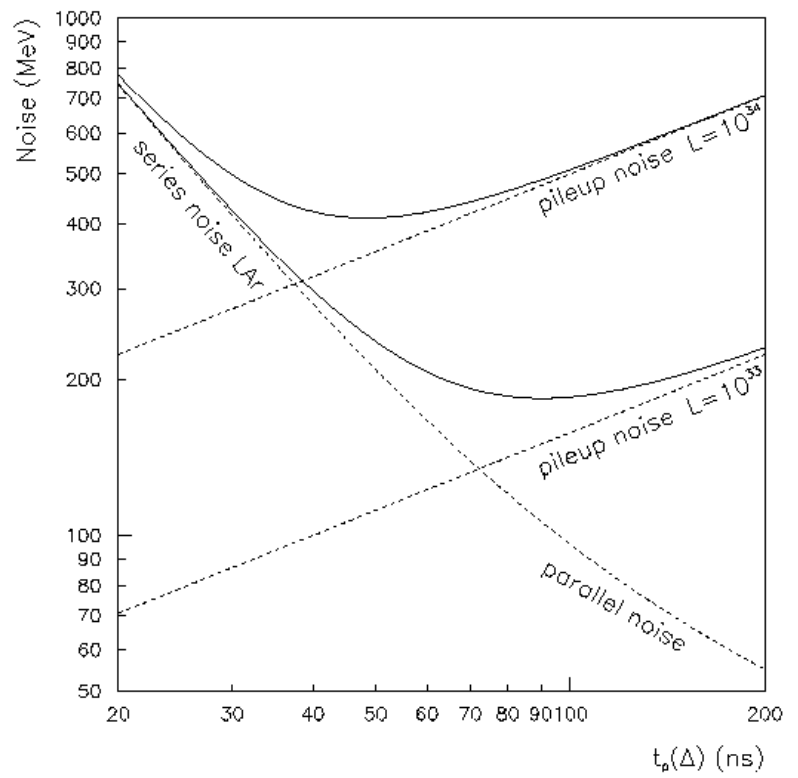
c the **constant term** (hits at high energy)
Essentially detector non homogeneities like intrinsic geometry, calibration but also energy leakage

NOISE TERM WITH PILE-UP

Electronics noise vs pile-up noise

Electronics integration time was optimized taking into account both contributions for LHC nominal luminosity if $10^{34}\text{cm}^{-2}\text{s}^{-1}$

Contribution from the noise to an electron is typically $\sim 300\text{-}400\text{ MeV}$ at such luminosity



THE CONSTANT TERM

The constant term describes the level of uniformity of response of the calorimeter as a function of **position**, **time**, **temperature** and which are not corrected for.

Geometry non uniformity

Non uniformity in electronics response

Signal reconstruction

Energy leakage

Dominant term at high energy

| Correlated contributions | Impact on uniformity | ATLAS LAr EMB testbeam |
|---------------------------|------------------------|------------------------|
| Calibration | 0.23% | |
| Readout electronics | 0.10% | |
| Signal reconstruction | 0.25% | |
| Monte Carlo | 0.08% | |
| Energy scheme | 0.09% | |
| Overall (data) | 0.38% (0.34%) | |
| Uncorrelated contribution | P13 | P15 |
| Lead thickness | 0.09% | 0.14% |
| Gap dispersion | 0.18% | 0.12% |
| Energy modulation | 0.14% | 0.10% |
| Time stability | 0.09% | 0.15% |
| Overall (data) | 0.26% (0.26%) | 0.25% (0.23%) |

CALORIMETERS

Detector for energy measurement via total absorption of particles

Principle of operation

Incoming particle initiates particle shower

Electromagnetic, hadronic

Shower properties depend on particle type and detector material

Energy is deposited in active regions

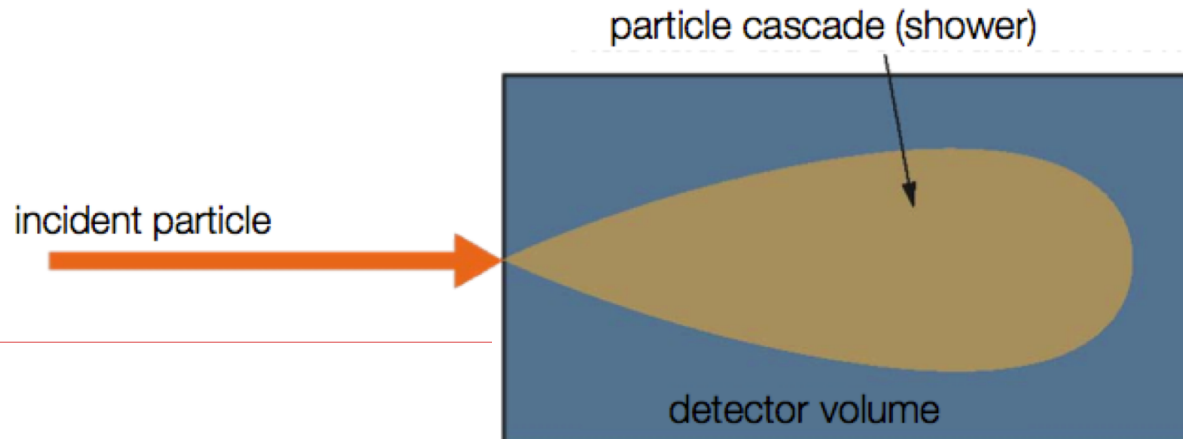
Heat, ionisation, atom excitation (scintillation), Cerenkov light

Different calorimeters use different kind of signal

Signal is proportional to energy released

Proportion \rightarrow calibration

Shower containment



CALORIMETERS CAN:

Calorimeters can be built as 4π -detectors

They can detect particles over almost the full solid angle

Magnetic spectrometers: anisotropy due to magnetic field

Calorimeters are often also sensitive to particle position

Important for neutral particles: no track in inner detector

Calorimeters can provide fast timing signal

0.1 to 10 ns

They can be used for triggering

Calorimeters can measure the energy of both charged and neutral particles

Magnetic spectrometer: only charged particles

Segmentation in depth allows particle separation

e.g. separate hadrons from particles which only interact electromagnetically

USEFUL QUANTITIES

Radiation length

$$X_0 \approx \frac{180A}{Z^2} \text{ g.cm}^{-2}$$

Radiation length
for a composite material

$$1/X_0 = \sum w_j / X_j$$

Moliere Radius

$$R_M = \frac{21\text{MeV} \times X_0}{E_c} \approx \frac{7A}{Z} \text{ g} \times \text{cm}^{-2}$$

Energy resolution

$$\frac{\sigma}{E} = \frac{a}{\sqrt{E}} \oplus \frac{b}{E} \oplus c$$

HOMOGENOUS CALORIMETERS

- ★ In a homogeneous calorimeter the whole detector volume is filled by a high-density material which simultaneously serves as absorber as well as as active medium ...

| Signal | Material |
|---------------------|--|
| Scintillation light | BGO, BaF ₂ , CeF ₃ , ... |
| Cherenkov light | Lead Glass |
| Ionization signal | Liquid noble gases (Ar, Kr, Xe) |

- ★ Advantage: homogenous calorimeters provide optimal energy resolution
- ★ Disadvantage: very expensive
- ★ Homogenous calorimeters are exclusively used for electromagnetic calorimeter, i.e. energy measurement of electrons and photons

SAMPLING CALORIMETERS

Principle:

Alternating layers of absorber and active material [sandwich calorimeter]

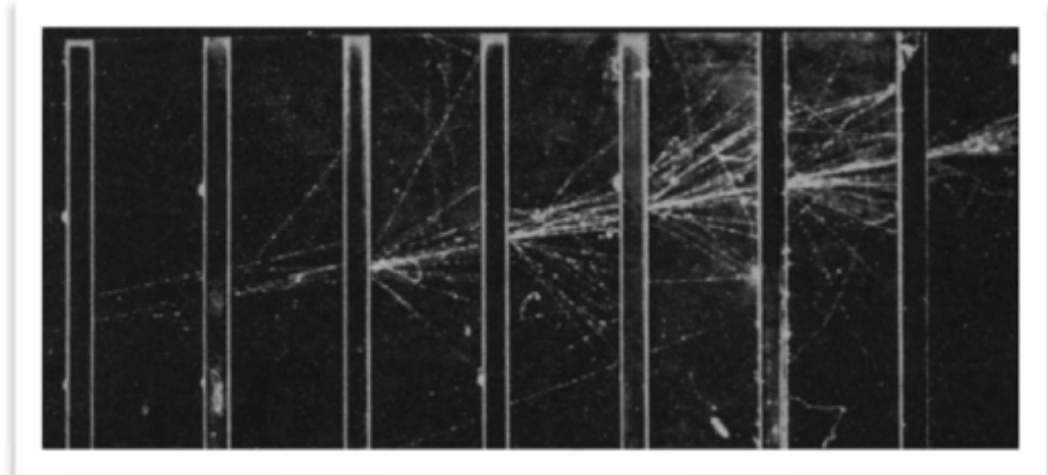
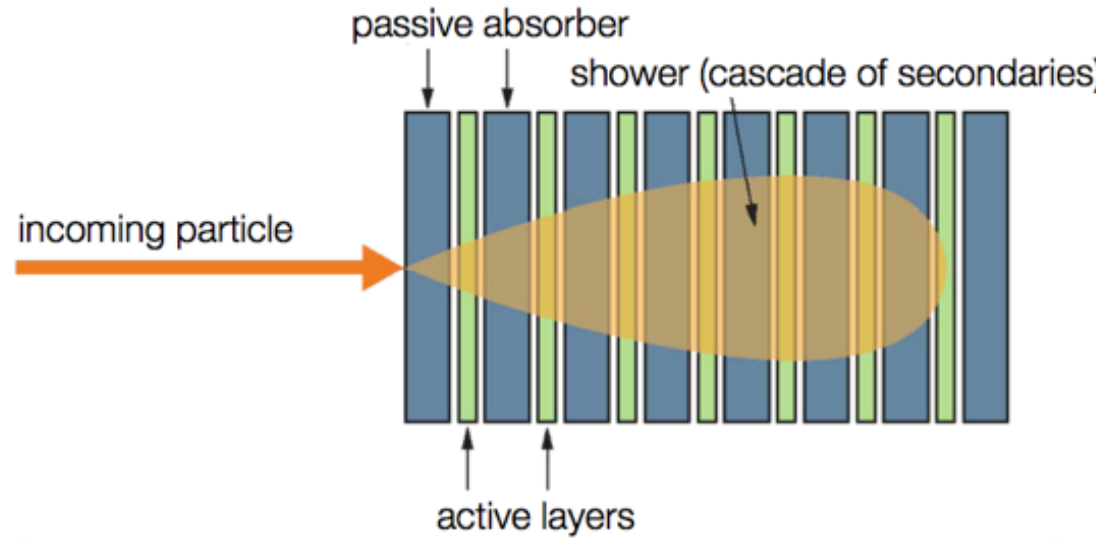
Absorber materials:
[high density]

- Iron (Fe)
- Lead (Pb)
- Uranium (U)
[For compensation ...]

Active materials:

- Plastic scintillator
- Silicon detectors
- Liquid ionization chamber
- Gas detectors

Scheme of a sandwich calorimeter



Electromagnetic shower

SAMPLING CALORIMETERS

★ Advantages:

By separating passive and active layers the different layer materials can be optimally adapted to the corresponding requirements ...

By freely choosing high-density material for the absorbers one can build very compact calorimeters ...

Sampling calorimeters are simpler with more passive material and thus cheaper than homogeneous calorimeters ...

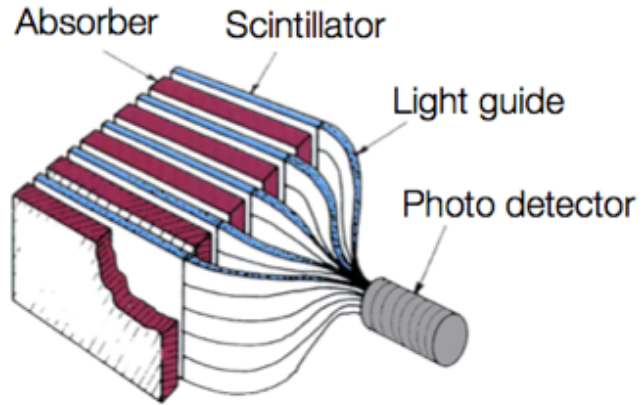
★ Disadvantages:

Only part of the deposited particle energy is actually detected in the active layers; typically a few percent [for gas detectors even only $\sim 10^{-5}$] ...

Due to this sampling-fluctuations typically result in a reduced energy resolution for sampling calorimeters ...

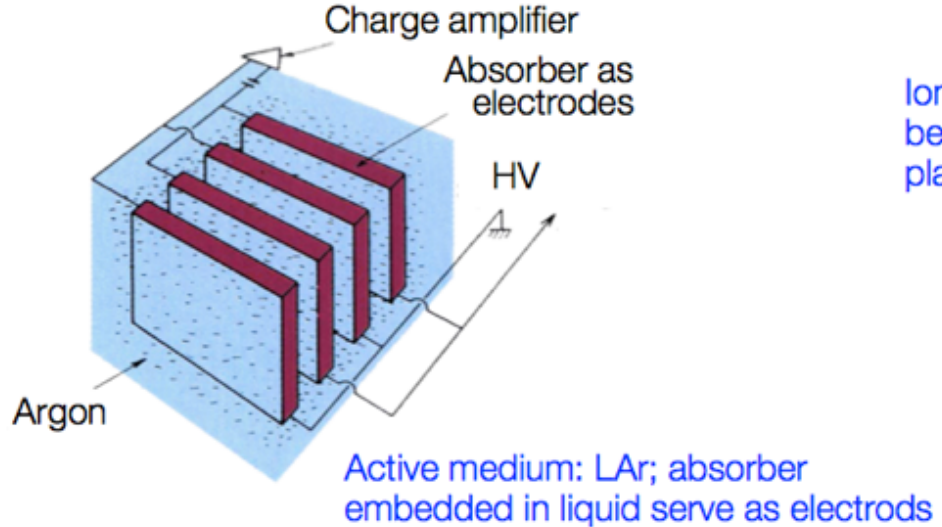
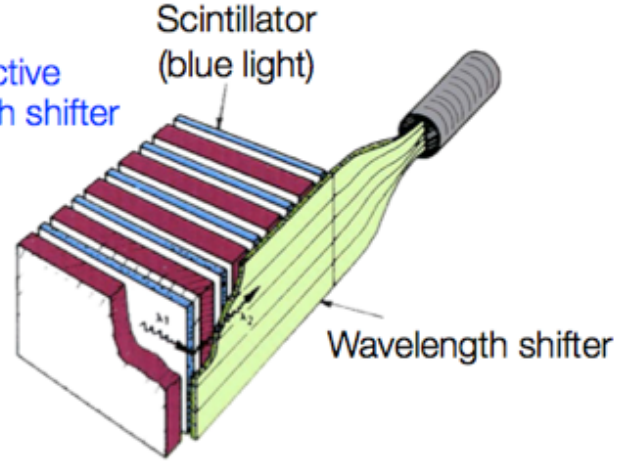
SAMPLING CALORIMETER

Scintillators as active layer;
signal readout via photo multipliers

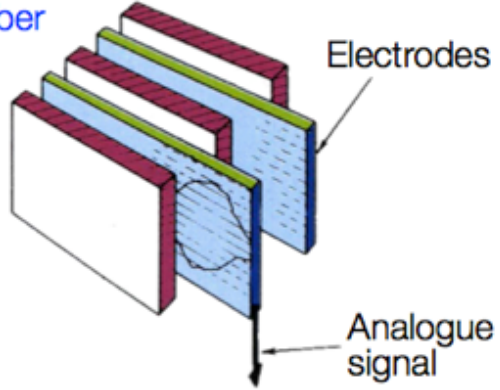


Possible setups

Scintillators as active layer; wave length shifter to convert light



Ionization chambers between absorber plates



HOMOGENEOUS vs SAMPLING CALORIMETERS

| Technology (Experiment) | Depth | Energy resolution | Date |
|--|---------------------|-----------------------------------|------|
| NaI(Tl) (Crystal Ball) | 20X ₀ | 2.7%/E ^{1/4} | 1983 |
| Bi ₄ Ge ₃ O ₁₂ (BGO) (L3) | 22X ₀ | 2%/√E ⊕ 0.7% | 1993 |
| CsI (KTeV) | 27X ₀ | 2%/√E ⊕ 0.45% | 1996 |
| CsI(Tl) (BaBar) | 16–18X ₀ | 2.3%/E ^{1/4} ⊕ 1.4% | 1999 |
| CsI(Tl) (BELLE) | 16X ₀ | 1.7% for E _γ > 3.5 GeV | 1998 |
| PbWO ₄ (PWO) (CMS) | 25X ₀ | 3%/√E ⊕ 0.5% ⊕ 0.2/E | 1997 |
| Lead glass (OPAL) | 20.5X ₀ | 5%/√E | 1990 |
| Liquid Kr (NA48) | 27X ₀ | 3.2%/√E ⊕ 0.42% ⊕ 0.09/E | 1998 |
| Scintillator/depleted U (ZEUS) | 20–30X ₀ | 18%/√E | 1988 |
| Scintillator/Pb (CDF) | 18X ₀ | 13.5%/√E | 1988 |
| Scintillator fiber/Pb spaghetti (KLOE) | 15X ₀ | 5.7%/√E ⊕ 0.6% | 1995 |
| Liquid Ar/Pb (NA31) | 27X ₀ | 7.5%/√E ⊕ 0.5% ⊕ 0.1/E | 1988 |
| Liquid Ar/Pb (SLD) | 21X ₀ | 8%/√E | 1993 |
| Liquid Ar/Pb (H1) | 20–30X ₀ | 12%/√E ⊕ 1% | 1998 |
| Liquid Ar/depl. U (DØ) | 20.5X ₀ | 16%/√E ⊕ 0.3% ⊕ 0.3/E | 1993 |
| Liquid Ar/Pb accordion (ATLAS) | 25X ₀ | 10%/√E ⊕ 0.4% ⊕ 0.3/E | 1996 |

Homogeneous

Sampling

Resolution of typical electromagnetic calorimeter [E is in GeV]

Hadronic Showers

Hadron showers

Hadronic cascades develop in an analogous way to e.m. showers

Strong interaction controls overall development

High energy hadron interacts with material, leading to multi-particle production of more hadrons

These in turn interact with further nuclei

Nuclear breakup and spallation neutrons

Multiplication continues down to the pion production threshold

$$E \sim 2m_{\pi} = 0.28 \text{ GeV}/c^2$$

Neutral pions result in an electromagnetic component (immediate decay: $\pi^0 \rightarrow \gamma\gamma$) (also: $\eta \rightarrow \gamma\gamma$)

Energy deposited by:

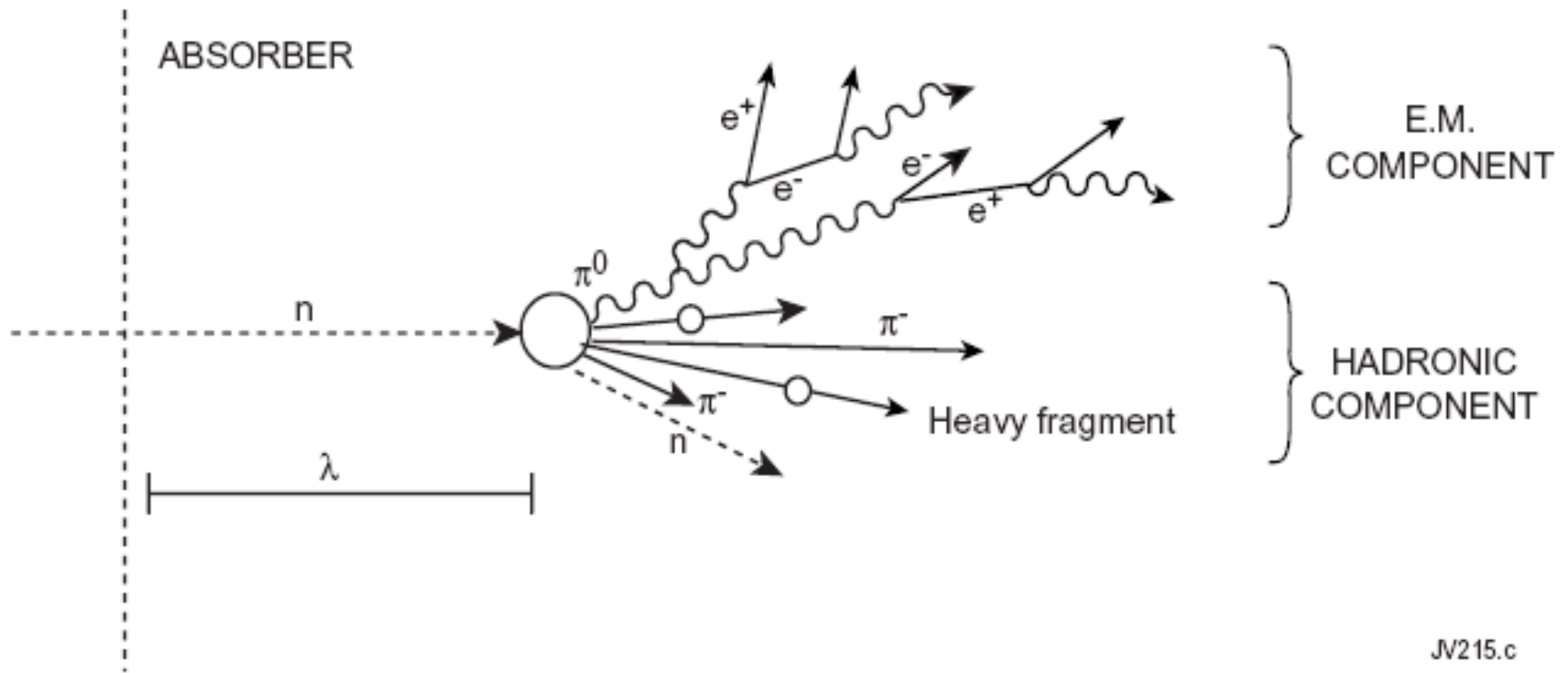
Electromagnetic component (i.e. as for e.m. showers)

Charged pions or protons

Low energy neutrons

Energy lost in breaking nuclei (nuclear binding energy)

Hadronic cascade



JV215.c

As compared to electromagnetic showers, hadron showers are:

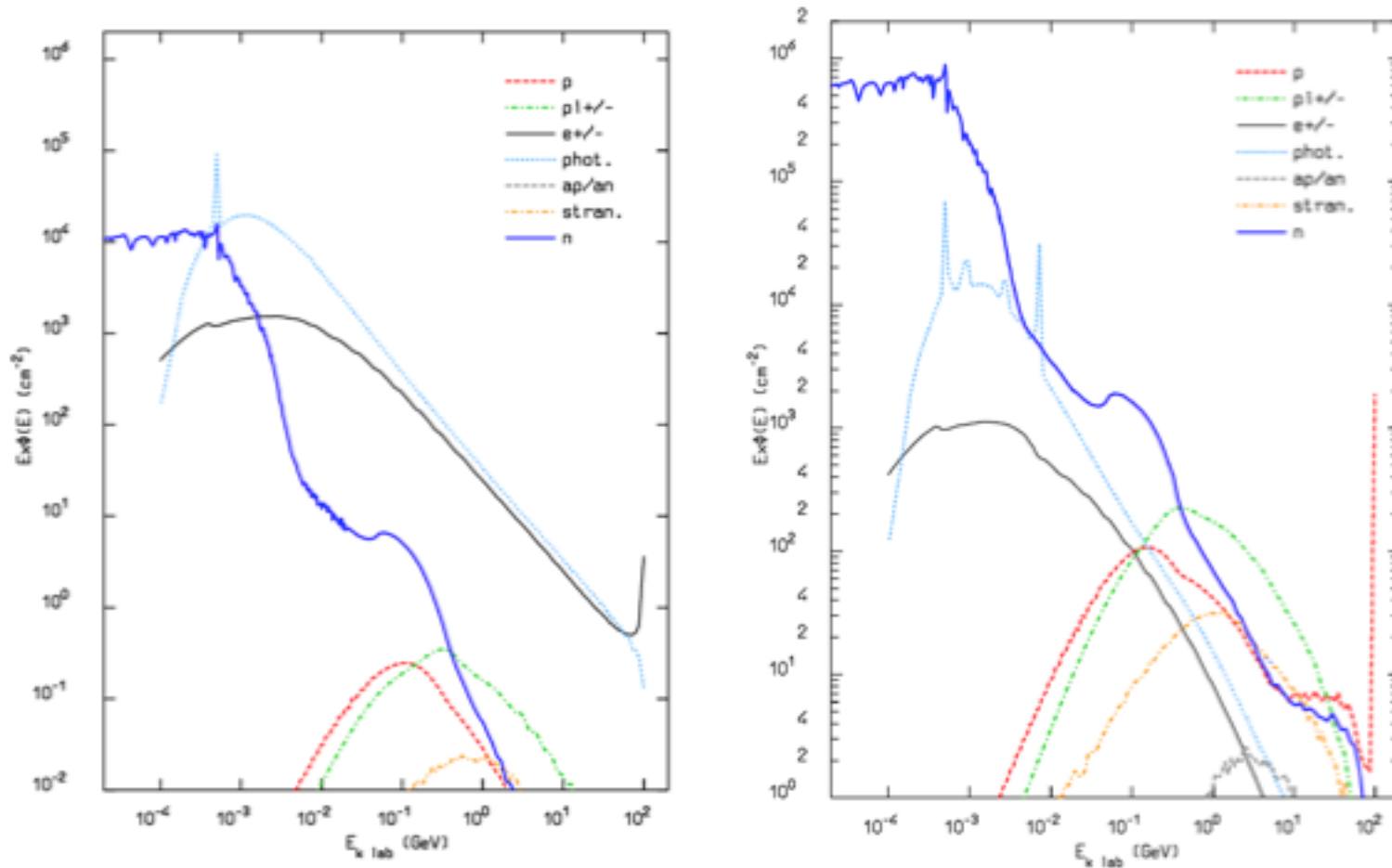
- Larger/more penetrating
- Subject to larger fluctuations – more erratic and varied

Hadronic Showers: Where does the energy go?

| | <i>Lead</i> | <i>Iron</i> |
|--|---------------|--------------|
| Ionization by pions | 19% | 21% |
| Ionization by protons | 37% | 53% |
| <i>Total ionization</i> | 56% | 74% |
| Nuclear binding energy loss | 32% | 16% |
| Target recoil | 2% | 5% |
| <i>Total invisible energy</i> | 34% | 21% |
| Kinetic energy evaporation neutrons | 10% | 5% |
| Number of charged pions | 0.77 | 1.4 |
| Number of protons | 3.5 | 8 |
| Number of cascade neutrons | 5.4 | 5 |
| Number of evaporation neutrons | 31.5 | 5 |
| Total number of neutrons | 36.9 | 10 |
| Neutrons/protons | 10.5/1 | 1.3/1 |

Em vs HAD shower development

These spectra are dominated by electrons, positrons, photons, and neutrons at low energy. The structure in the photon spectrum at approximately 8 MeV reflects an (n, γ) reaction and is a fingerprint of nuclear physics; the line at 511 keV results from $e+e-$ annihilation photons. These low-energy spectra encapsulate all the information relevant to the hadronic energy measurement.



$E[\text{GeV}]$

Hadronic shower development

Simple model of interaction on a disk of radius R: $\sigma_{\text{int}} = \pi R^2 \propto A^{2/3}$

$$\sigma_{\text{inel}} \approx \sigma_0 A^{0.7}, \quad \sigma_0 = 35 \text{ mb}$$

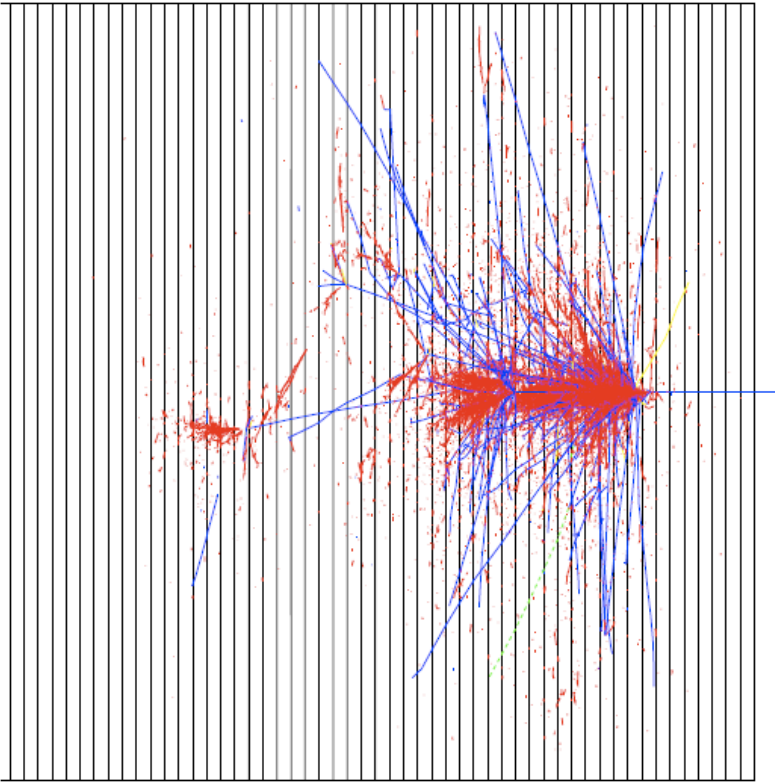
Nuclear interaction length: mean free path before inelastic interaction

$$\lambda_{\text{int}} \approx \frac{A}{N_A \sigma_{\text{int}}} \approx 35 A^{1/3} \text{ g cm}^{-2}$$

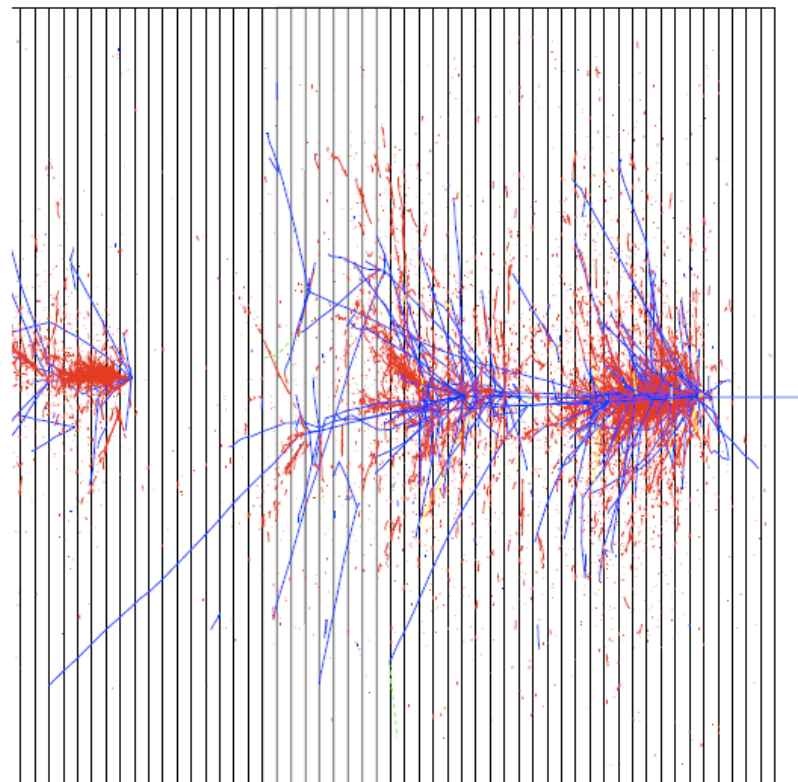
| | Z | ρ (g.cm ⁻³) | E_c (MeV) | X_0 (cm) | λ_{int} (cm) |
|-------------------|----|---------------------------------|----------------|---------------|--------------------------------|
| Air | | | | 30 420 | ~70 000 |
| Water | | | | 36 | 84 |
| PbWO ₄ | | 8.28 | | 0.89 | 22.4 |
| C | 6 | 2.3 | 103 | 18.8 | 38.1 |
| Al | 13 | 2.7 | 47 | 8.9 | 39.4 |
| L Ar | 18 | 1.4 | | 14 | 84 |
| Fe | 26 | 7.9 | 24 | 1.76 | 16.8 |
| Cu | 29 | 9 | 20 | 1.43 | 15.1 |
| W | 74 | 19.3 | 8.1 | 0.35 | 9.6 |
| Pb | 82 | 11.3 | 6.9 | 0.56 | 17.1 |
| U | 92 | 19 | 6.2 | 0.32 | 10.5 |

Hadron showers

1.



2.



red - e.m. component
blue - charged hadrons

- Individual hadron showers are quite dissimilar

Hadron shower longitudinal profiles

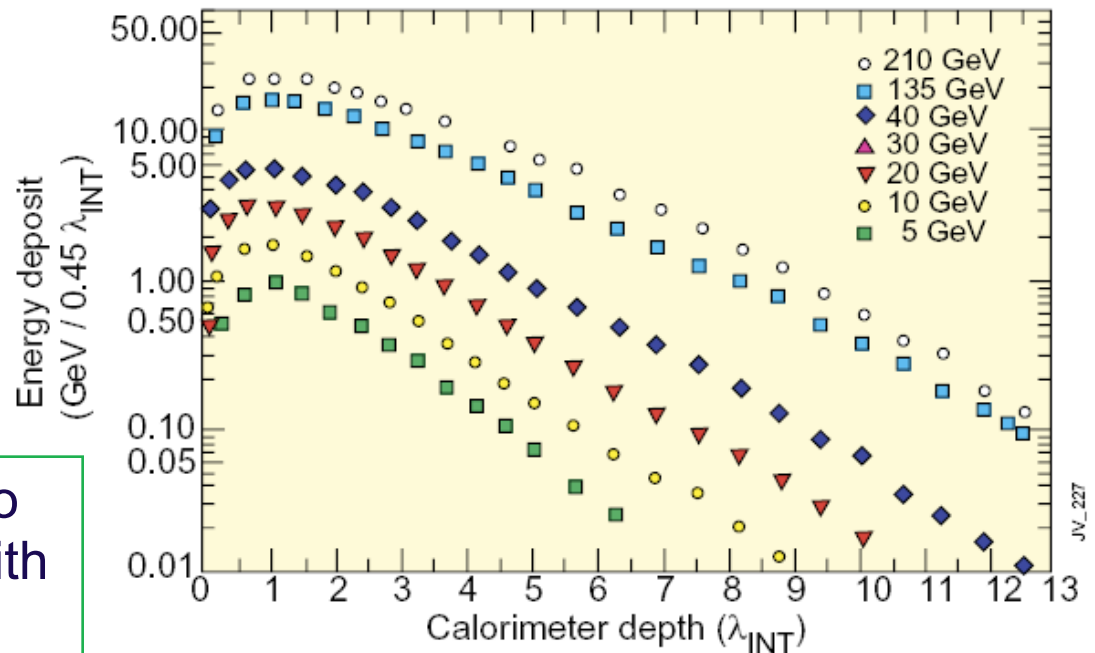
Longitudinal profile

Initial peak from π^0 s produced in the first interaction

Gradual falloff characterised by the nuclear interaction length,

λ_{int}

WA78 : 5.4λ of 10mm U / 5mm Scint + 8λ of 25mm Fe / 5mm Scint



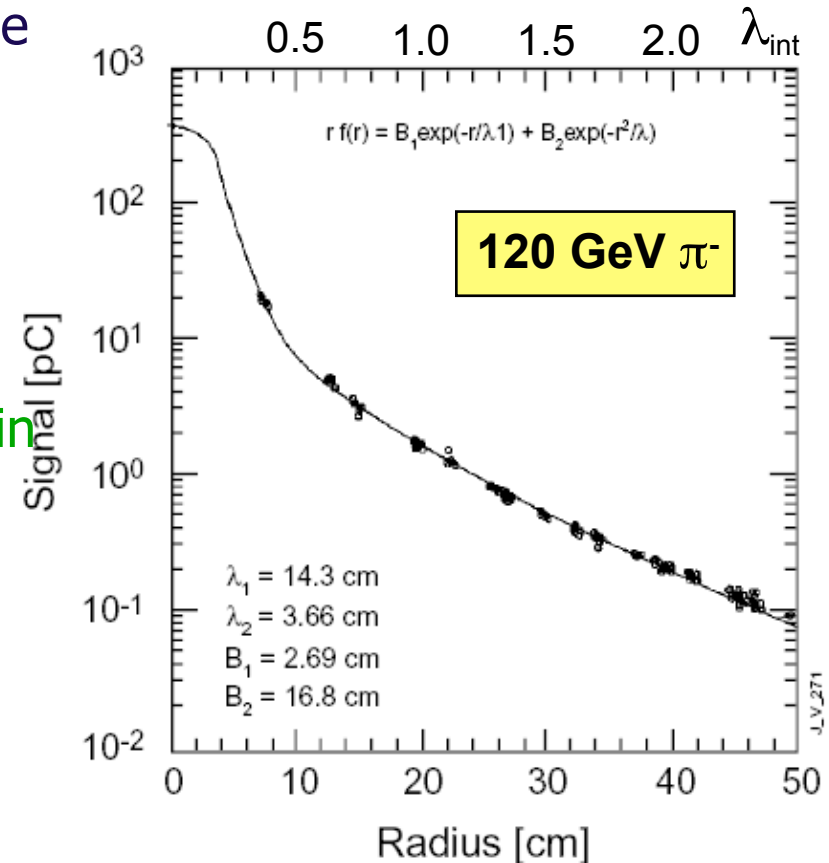
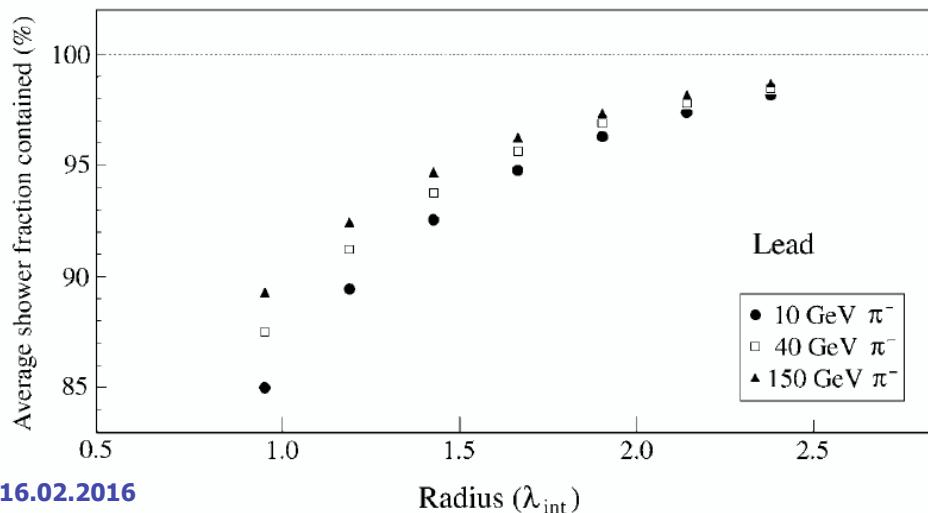
As with e.m. showers: depth to contain a shower increases with $\log(E)$

Hadron shower transverse profiles

Mean transverse momentum from interactions, $\langle p_T \rangle \sim 300$ MeV, is about the same magnitude as the energy lost traversing 1λ for many materials

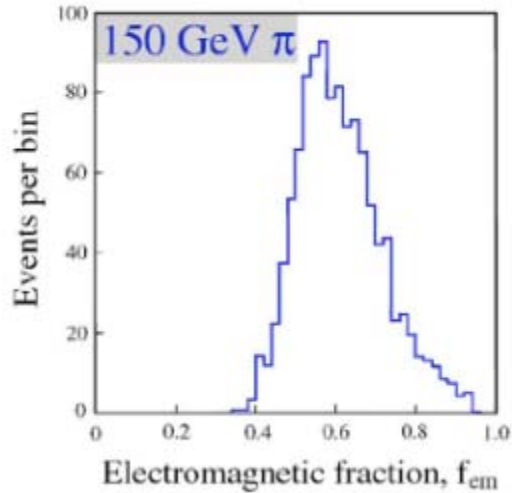
So radial extent of the cascade is well characterized by λ

The π^0 component of the cascade results in an electromagnetic core



Lateral containment increases with energy

Hadronic Showers: EM fraction

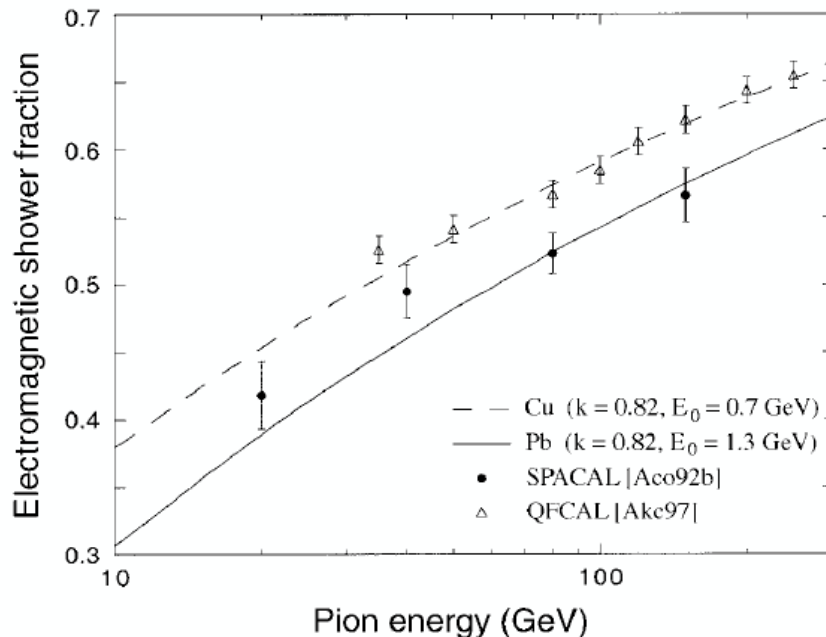


Large fluctuation of the EM component from one shower to the other

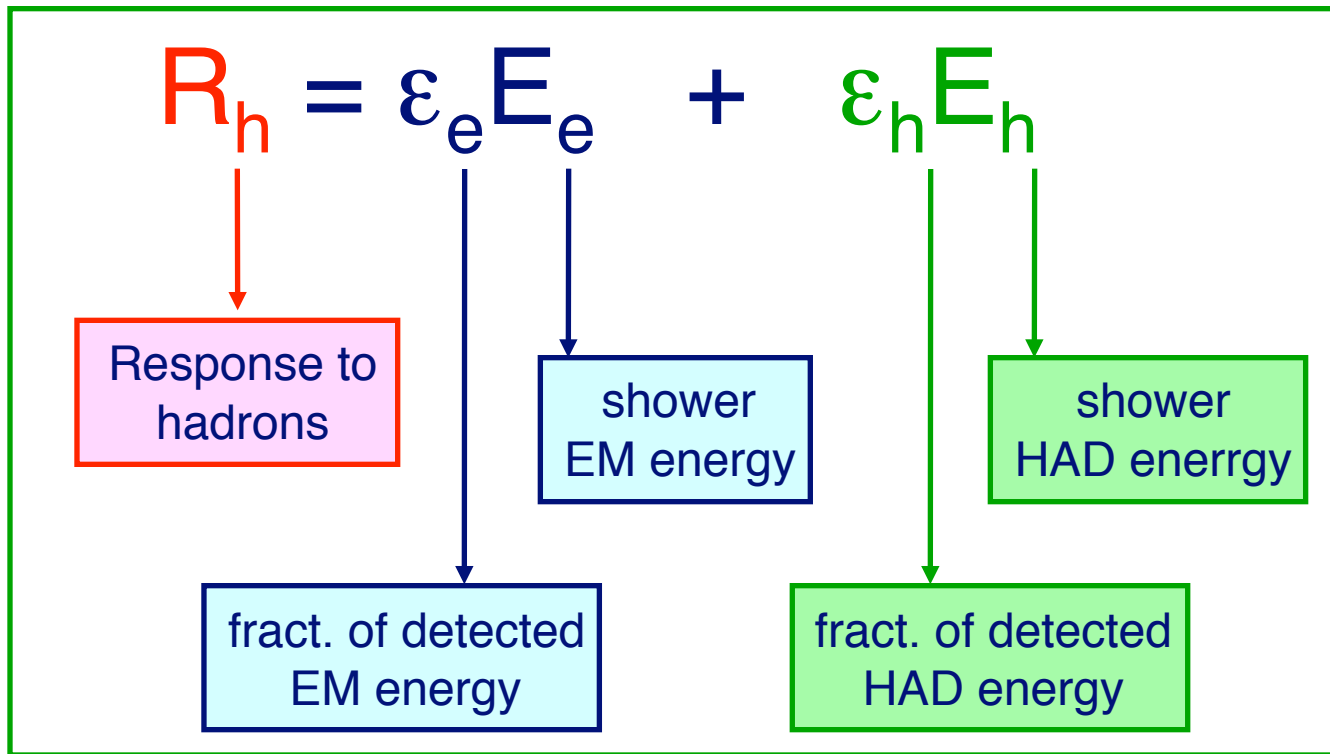
Varies with energy

Energy resolution is degraded w.r.t. EM showers

50-100%/ $\sqrt{E} \oplus$ a few %



Hadronic shower and non compensation

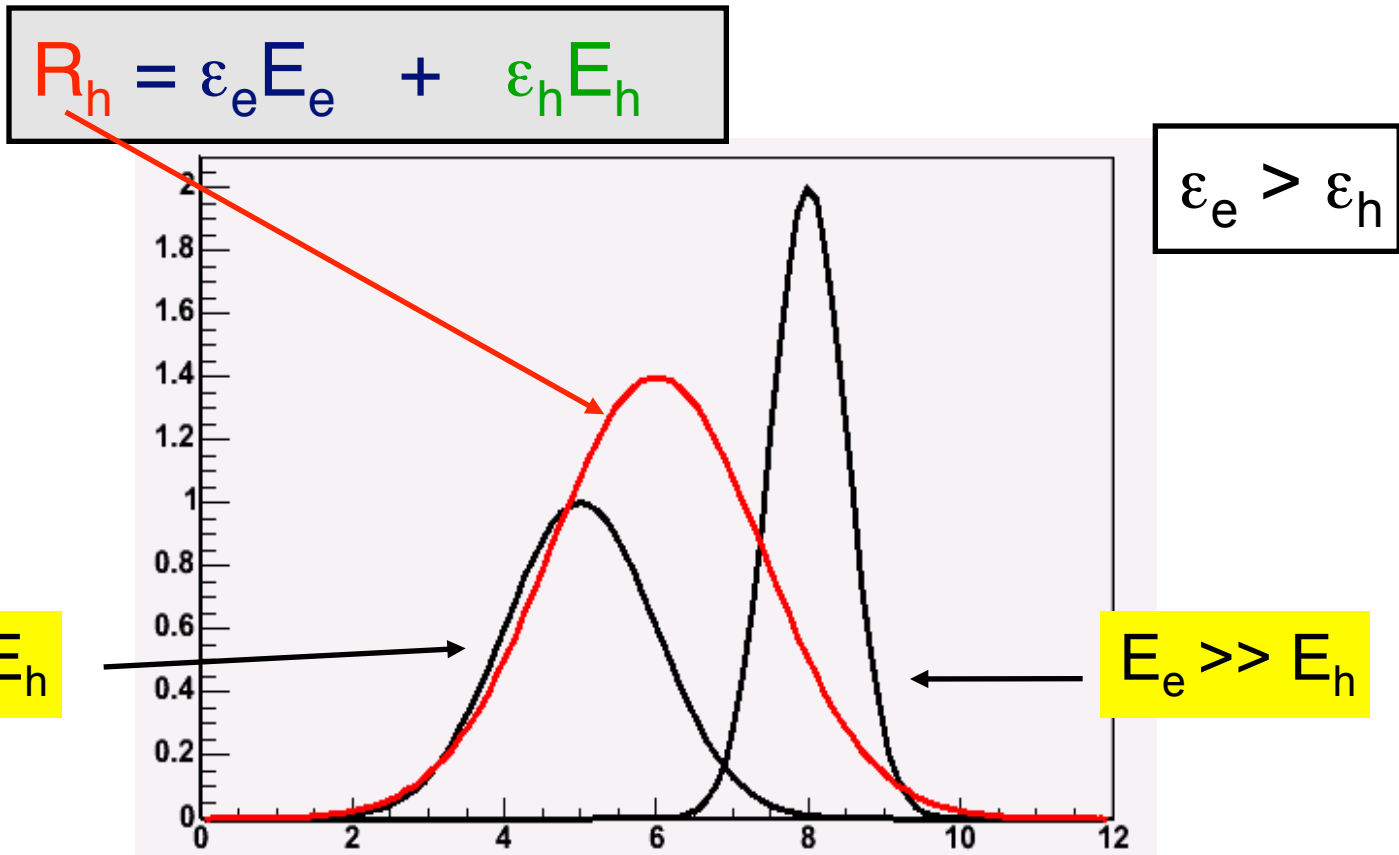


$$\frac{e}{h} = \frac{\epsilon_e}{\epsilon_h}$$

≈ 1 : compensating calorimeter

> 1 : non compensating calorimeter

Hadronic showers: non compensation



Jets

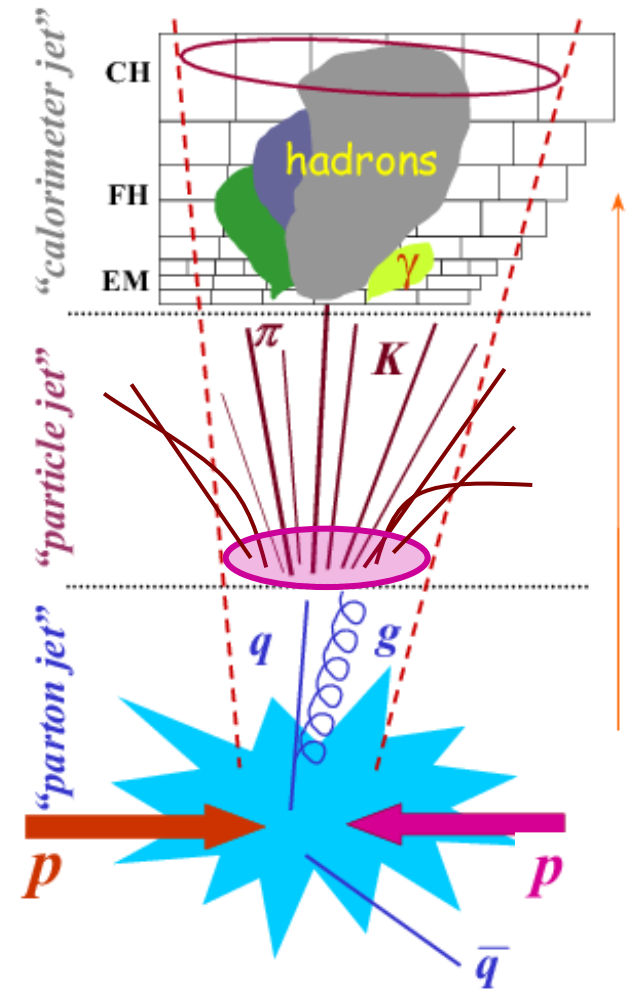
At Hadronic Colliders, quarks & gluons produced, evolves (parton shower, hadronisation) to become jets

In a cone around the initial parton:
high density of hadrons

LHC calorimeters cannot separate all the incoming hadrons

Use dedicated calibration schemes
(based on simulation in ATLAS)

Use tracking system to identify
charged hadrons (Particle Flow in
CMS)

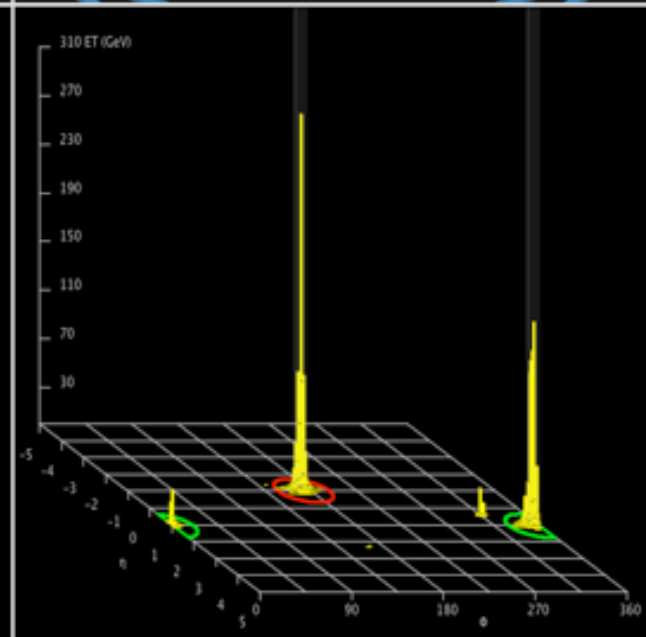
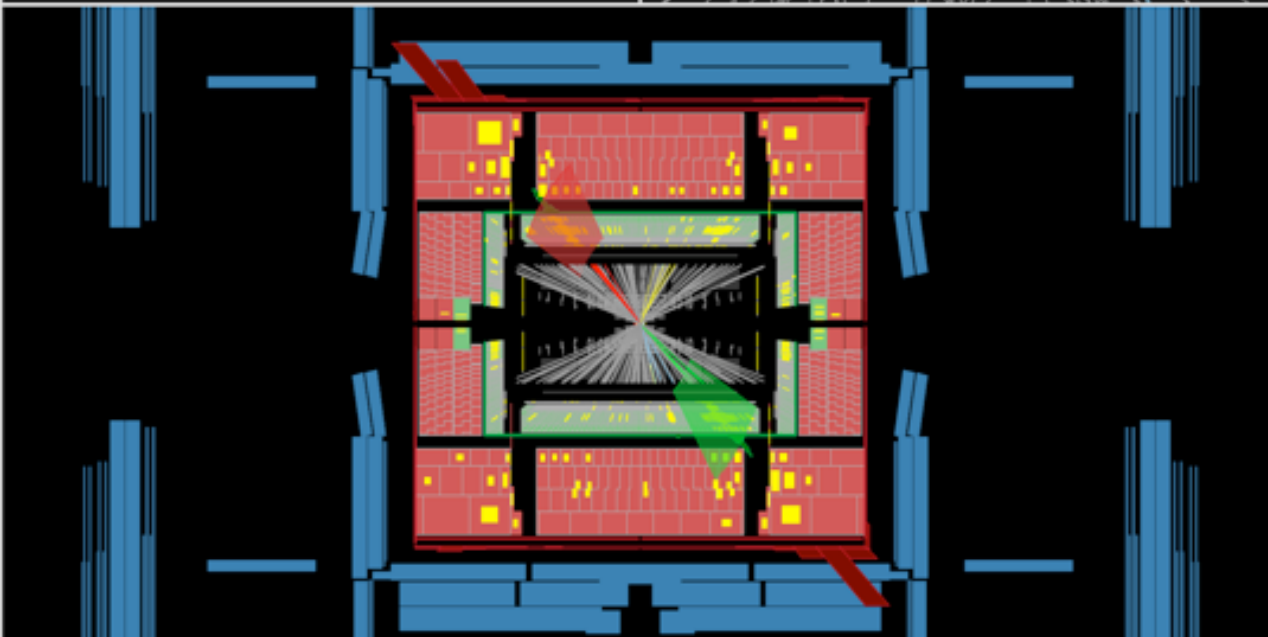
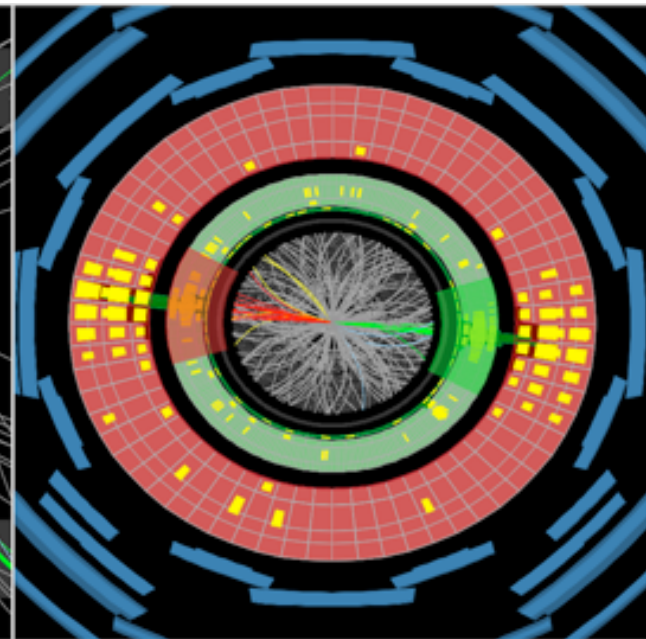
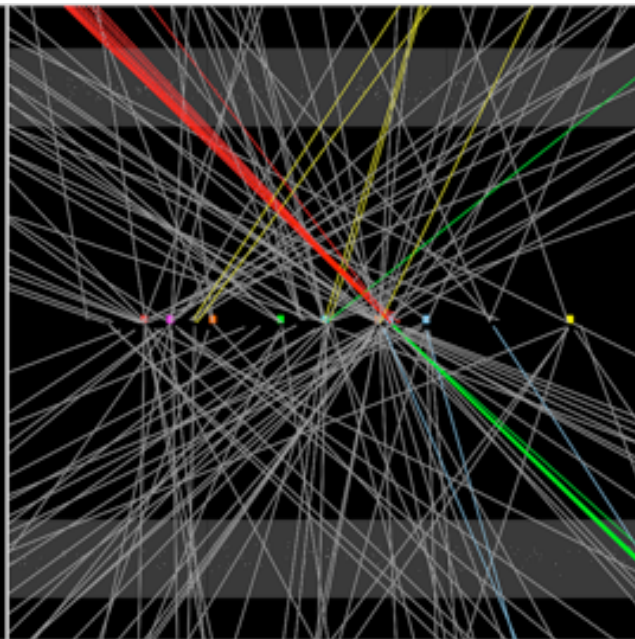




ATLAS EXPERIMENT

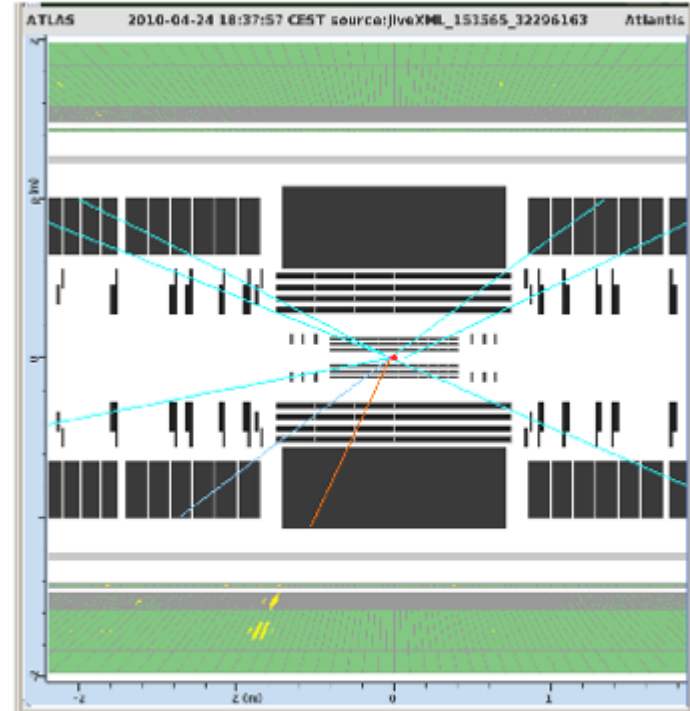
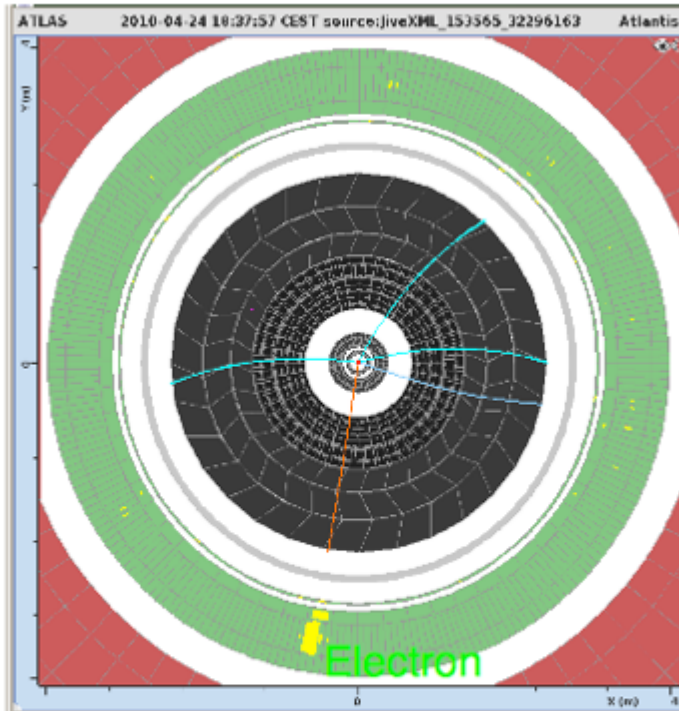
Run Number: 201269, Event Number: 80898559

Date: 2012-04-14 22:30:13 CEST



Missing Transverse Energy

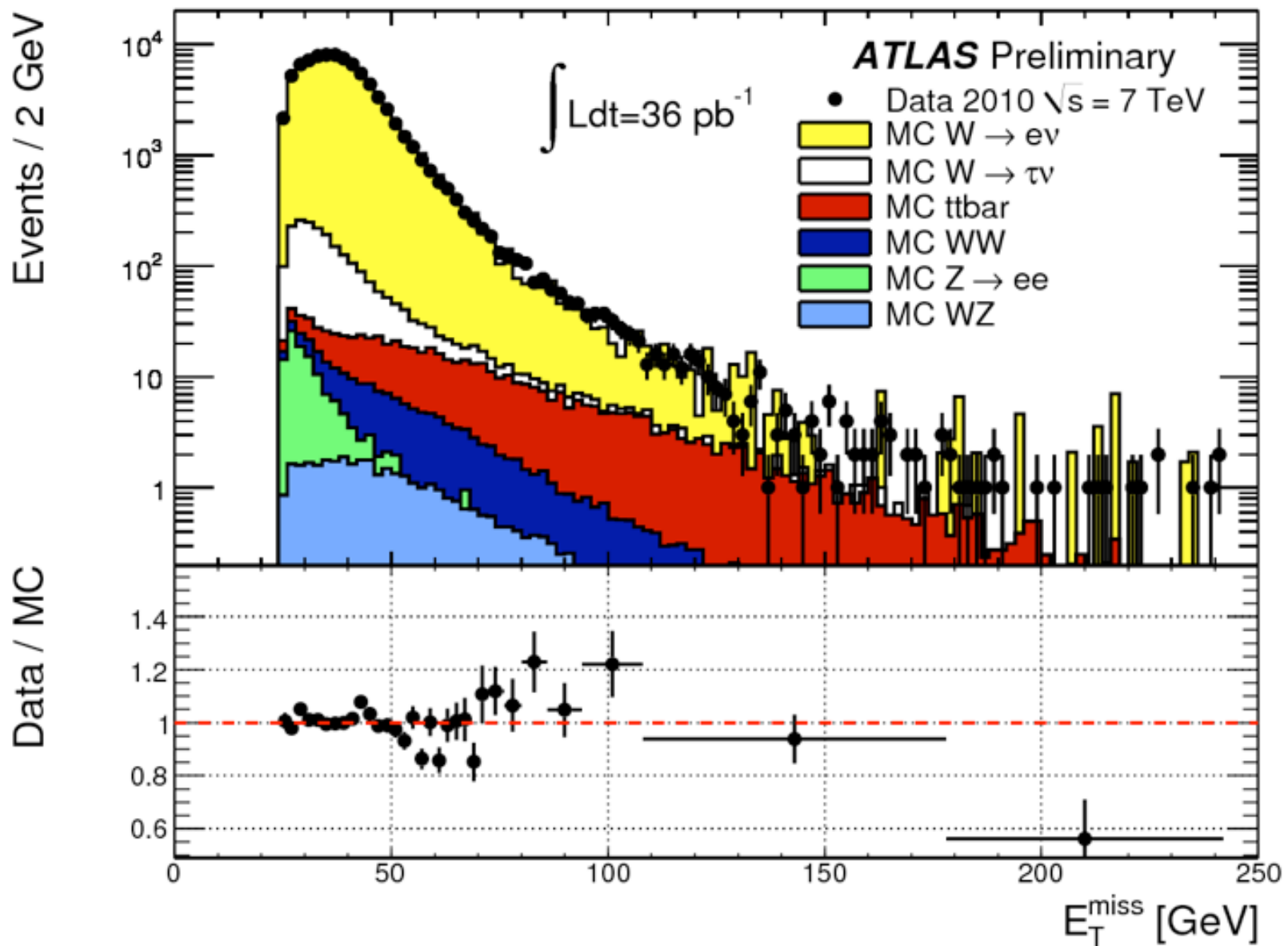
Missing transverse energy : $W \rightarrow e \nu$ candidate



- high pt electron (pt = 29 GeV); several low pt tracks (< 1 GeV)
- transverse momentum is a tool for selecting events in which a W boson has occurred
- the total transverse momentum vector is not balanced \implies missing energy
- the Missing Energy vector:
$$\vec{E}^{\text{miss}} = - \sum_{\text{calorimeter cells}} E_i \vec{u}_i$$

where \vec{u}_i is the unit vector between the collision point and the position of the energy deposition observed in the i^{th} cell of the calorimeter

ATLAS E_T^{miss} calibration



Interlude: muons

Muons interacting with matter

Muons are like electrons but behave differently when interacting with matter (at a given energy).

Bremsstrahlung process is $\sim 1/m^2$

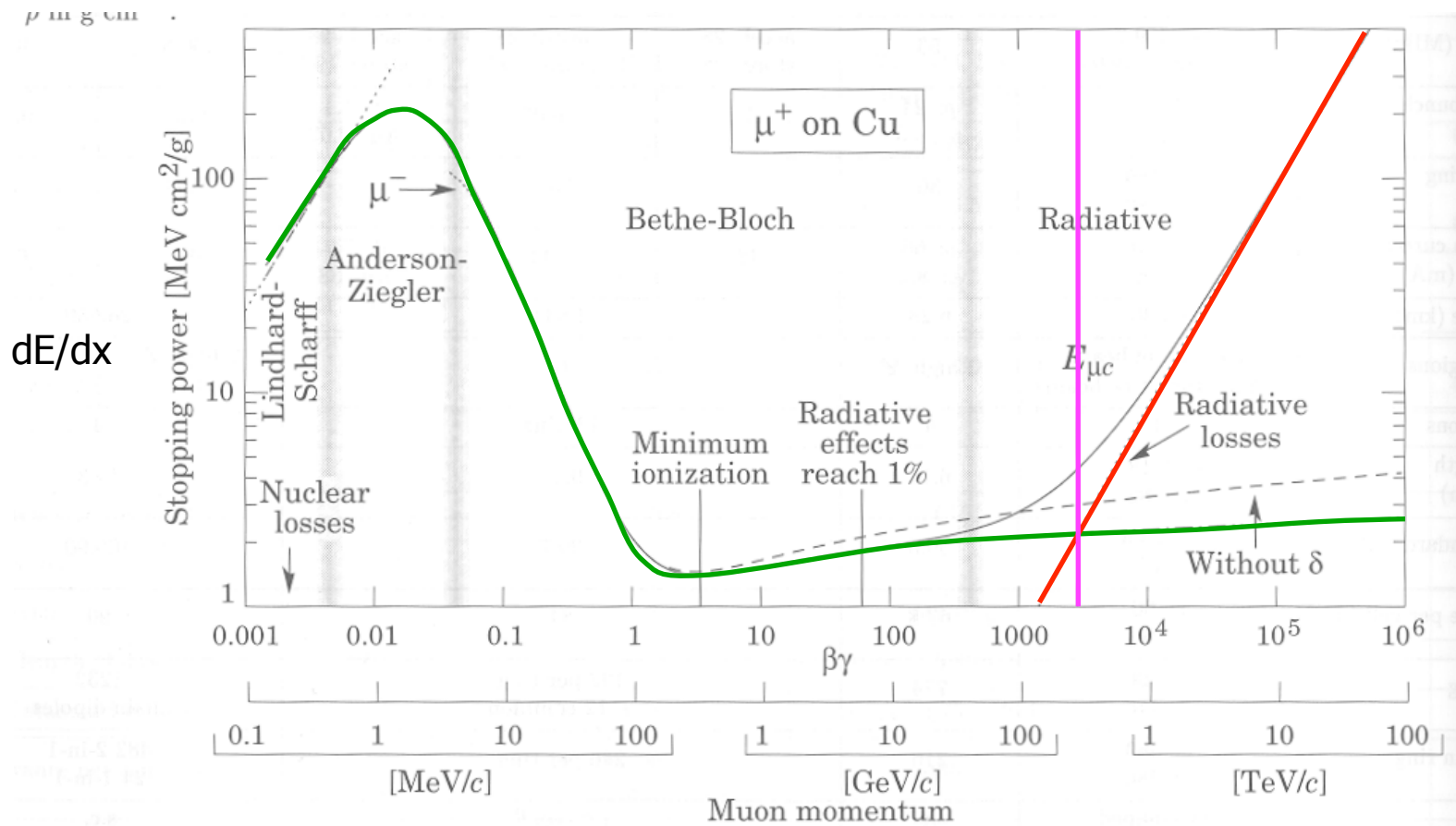
$$\left. \begin{array}{l} m_e = 0.519 \text{ MeV}/c^2 \\ m_\mu = 105,66 \text{ MeV}/c^2 \end{array} \right\} m_\mu / m_e \sim 200 \rightarrow (m_\mu / m_e)^2 \sim 40000$$

Contrary to electrons, muons ($E < 100 \text{ GeV}$) lose energy mainly via ionization with

$$E_c(\mu) = (m_\mu / m_e)^2 \times E_c(e)$$

$$E_c(\mu) \approx 200 \text{ GeV in lead}$$

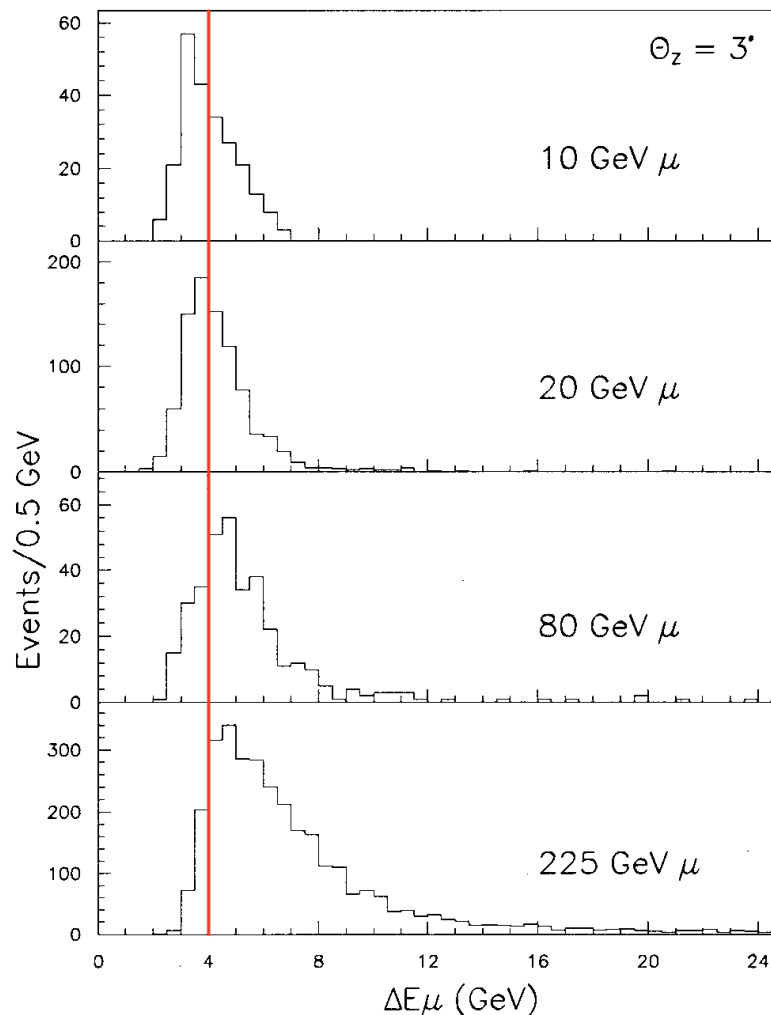
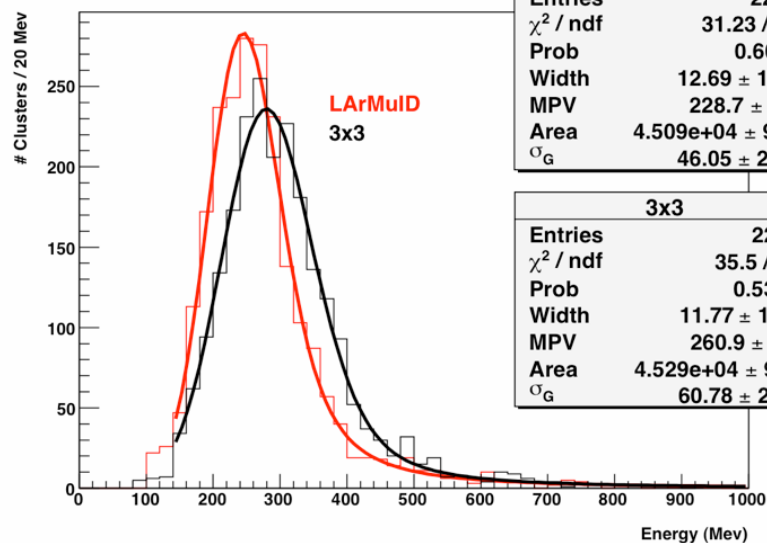
Muons in matter



Energy deposit of muons in matter

Muons energy deposit in matter is not proportional to their energy.

Cluster Energy ($0.3 < |\eta| < 0.4$)



Cosmic μ in ATLAS LAr EM barrel

Muons for calorimeters

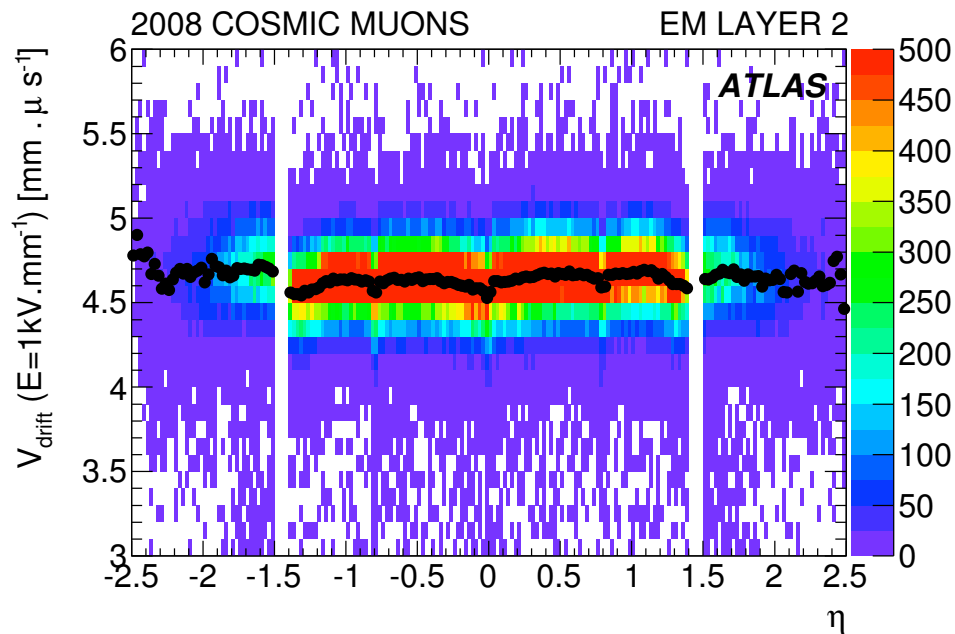
Muons deposit very little energy in calorimeter: $dE/dx \cdot x$

Except for catastrophic energy loss (γ emission)

They are nice tools to assess calorimeter response uniformity

at low energy

They are nice clean probes to analyse the calorimeter geometry



(b) Drift velocity

ELECTROMAGNETIC INTERACTIONS OF PARTICLES WITH MATTER

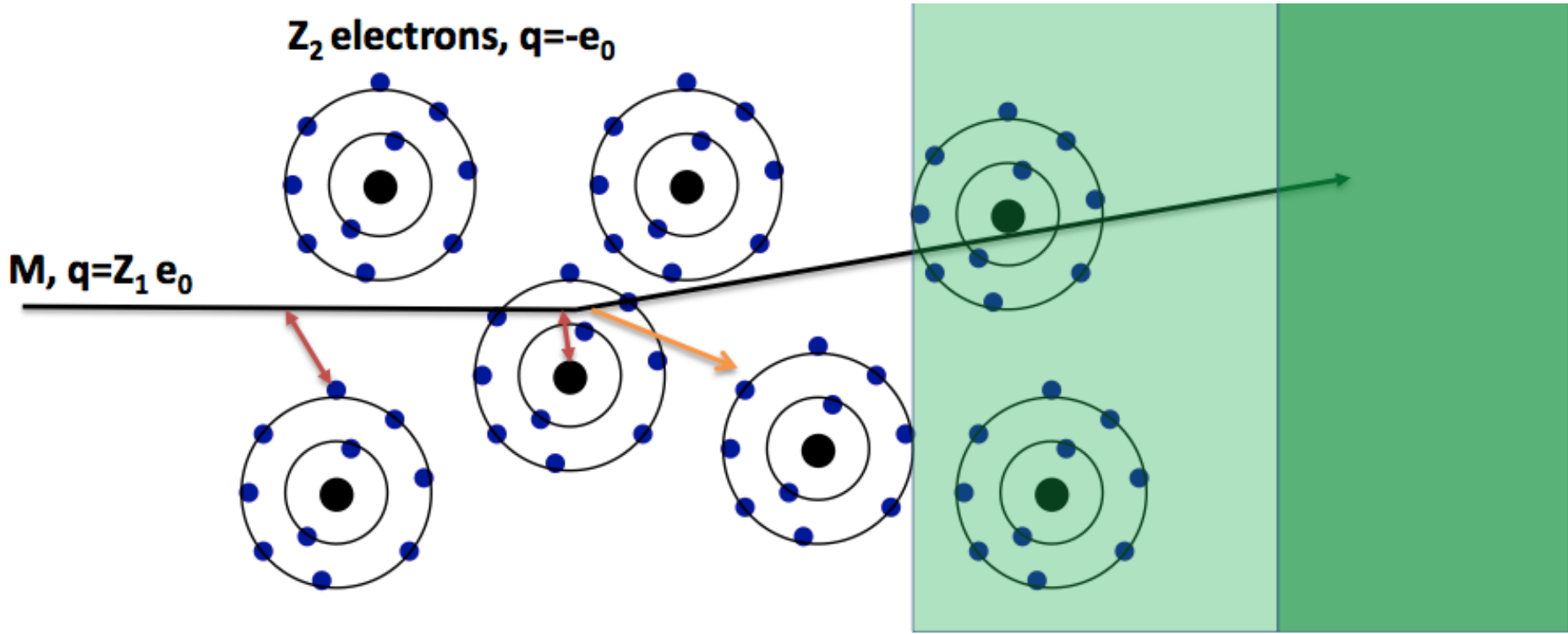
INTERACTIONS



DETECTORS

Z_2 electrons, $q=-e_0$

$M, q=Z_1 e_0$



Interaction with the atomic electrons.

The incoming particle loses energy and the atoms are **excited** or **ionised**.

Interaction with the atomic nucleus.

The incoming particle is deflected causing **multiple scattering** of the particle in the material. During this scattering a **Bremsstrahlung photon** can be emitted

In case the particle's velocity is larger than the velocity of light in the medium, the resulting EM shockwave manifests itself as **Cherenkov radiation**.

When the particle crosses the boundary between two media, there is a probability of 1% to produce an Xray photon called **Transition radiation**.

INTERACTIONS OF PARTICLES WITH MATTER

IONISATION AND EXCITATION

Charged particles traversing material and exciting and ionising atoms.

The average energy loss of the incoming particle by the process is to a good approximation described by the Bethe-Block formula.

CHERENKOV RADIATION

If a particle propagates in a material with velocity $>$ speed of light in this material, C radiation is emitted at a characteristic angle that depends on the particle velocity and the refractive index of the medium

TRANSITION RADIATION

If a charged particle is crossing the boundary between two materials of different dielectric permittivity, there is a certain probability for emission of an X-ray photon.

MULTIPLE SCATTERING AND BREMSSTRAHLUNG

Incoming particles are scattering off the atomic nuclei which are partially shielded by the atomic electrons.

This scattering imposes a lower level on the momentum resolution of the spectrometer, when measuring the particle momentum by deflection of the particle trajectory in the magnetic field.

The deflection of the particle on the nucleus results in an acceleration that causes the emission of Bremsstrahlung photons.

The photons in turn produce e^+e^- pairs in the vicinity of the nucleus, which causes the EM cascade.

This effect depends on m^{-2} : only relevant for electrons.

HADRONIC INTERACTION

Incoming hadrons on a material will interact with the nucleus and create a shower composed of hadrons, electrons, photon.

A fraction of the energy is *lost* in the form of binding energy or neutrinos.

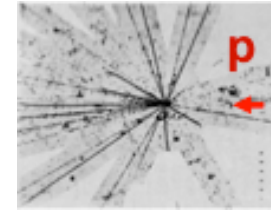
INTERACTIONS



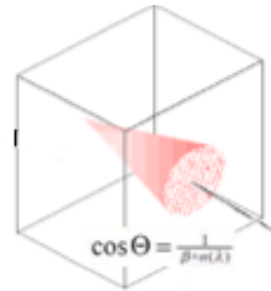
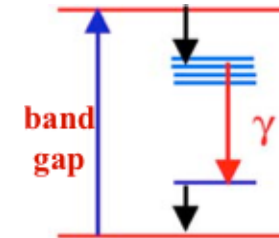
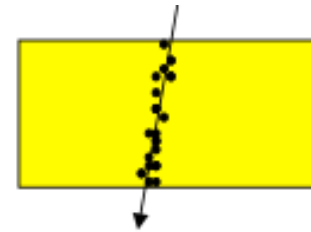
DETECTORS

FOUR STEPS

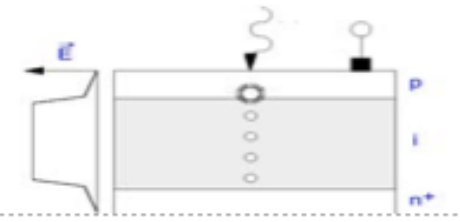
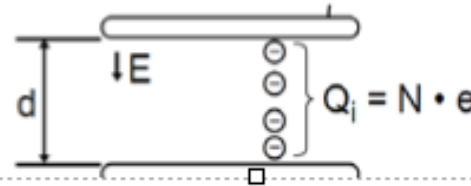
1. Particles interact with matter
depends on particle and material



2. Energy loss transfer to detectable signal
depends on the material



3. Signal collection
depends on signal and type of detection



4. BUILD a SYSTEM
depends on physics, experimental conditions,....



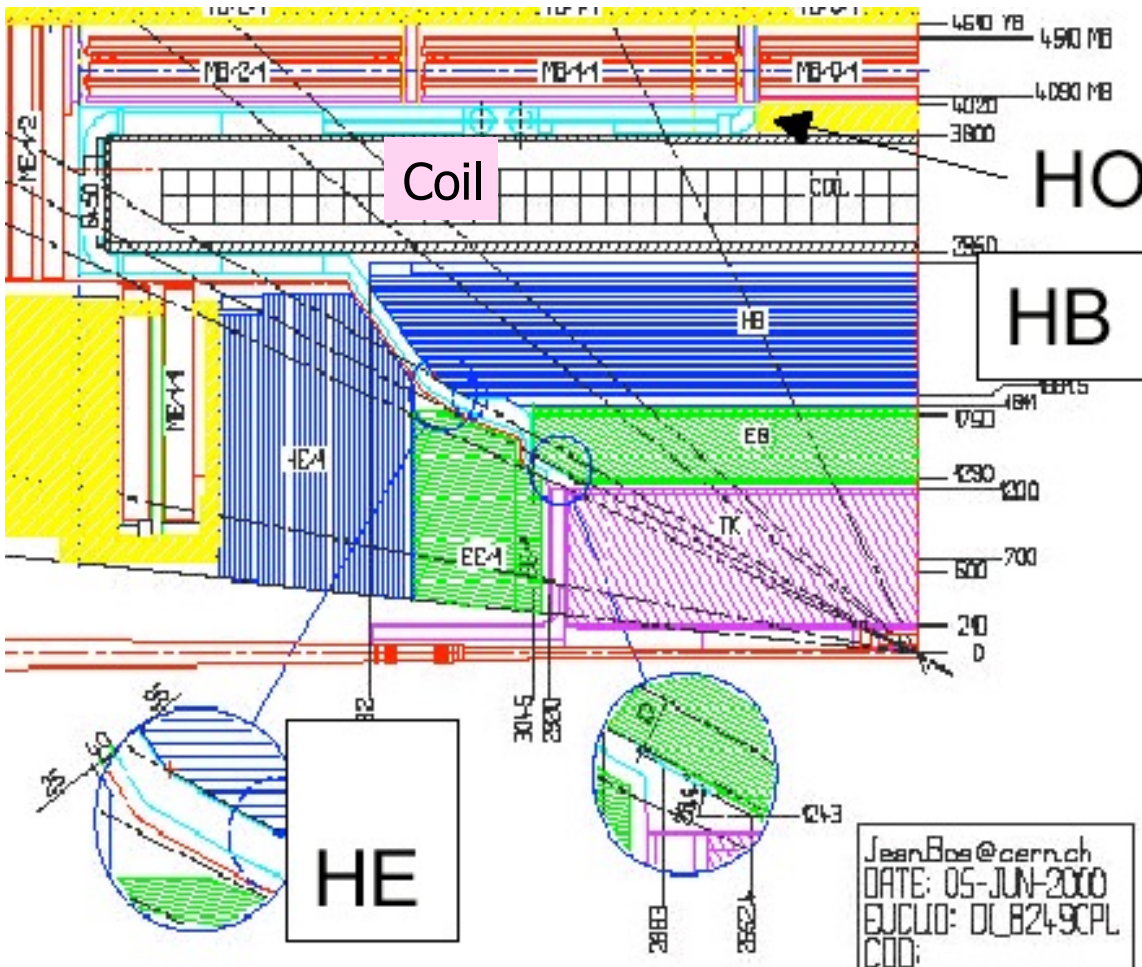
Two Examples

CMS

ATLAS

CMS calorimeter

The CMS calorimeter



The CMS choices

Solenoidal Magnetic Field: 4T
Outside the calorimeter

“Compact” calorimeter

Very precise EM calorimeter

PbWO crystal (very dense)

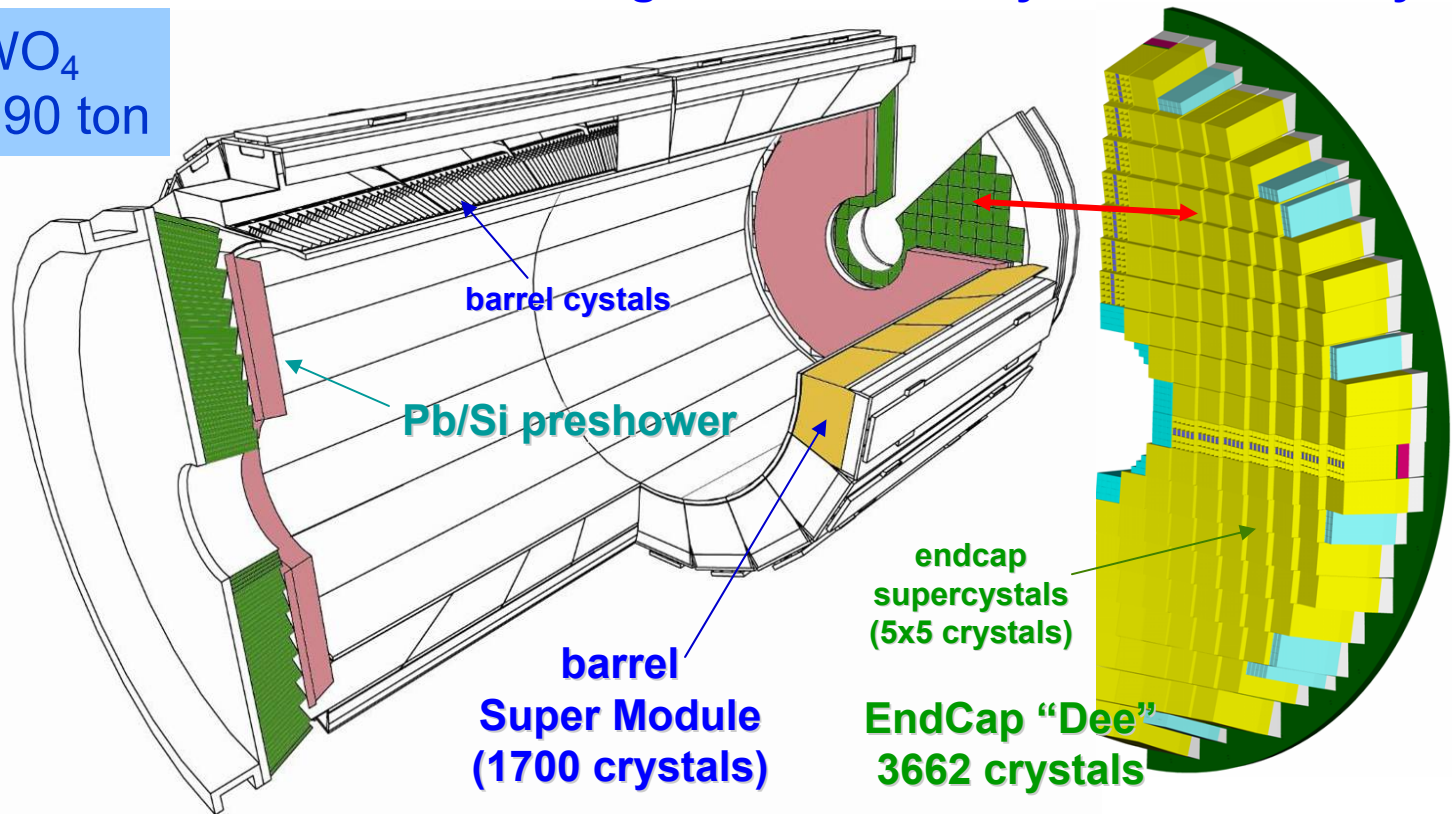
“Thin” HAD calorimeter

ECAL @ CMS

Precision electromagnetic calorimetry: 75848 PWO crystals

PWO: PbWO_4
about 10 m³, 90 ton

Previous
Crystal
calorimeters:
max 1m³



Barrel: $|\eta| < 1.48$
36 Super Modules
61200 crystals (2x2x23cm³)

EndCaps: $1.48 < |\eta| < 3.0$
4 Dees
14648 crystals (3x3x22cm³)

CMS crystals: PbWO_4



Excellent energy resolution

$X_0 = 0.89\text{cm} \rightarrow$ compact calorimeter (23cm for 26 X_0)

$R_M = 2.2\text{ cm} \rightarrow$ compact shower development

Fast light emission (80% in less than 15 ns)

Radiation hard (10^5Gy)

But

Low light yield (150 γ/MeV)

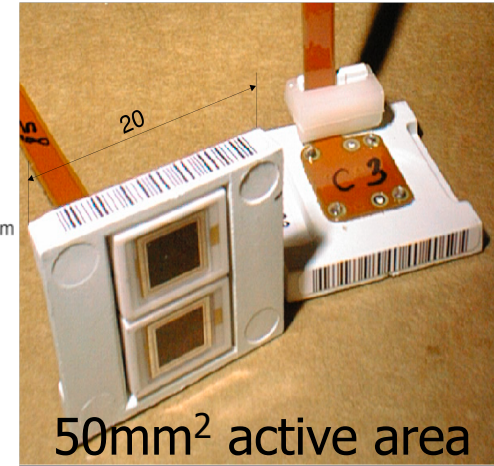
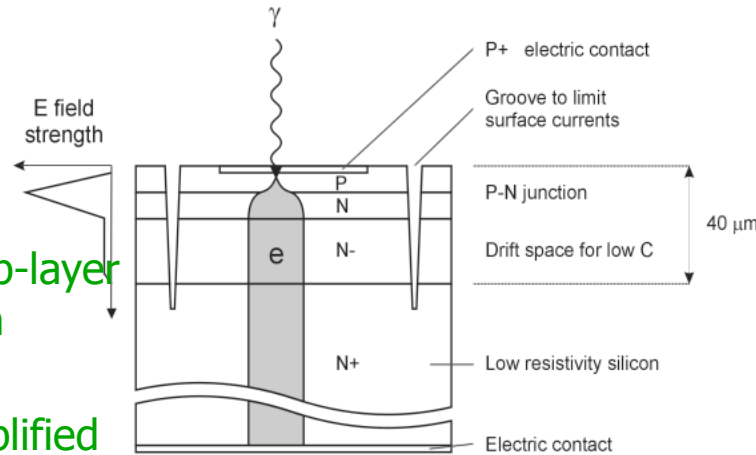
Response varies with dose

Response temperature dependence

Light Collection: APD & VPT

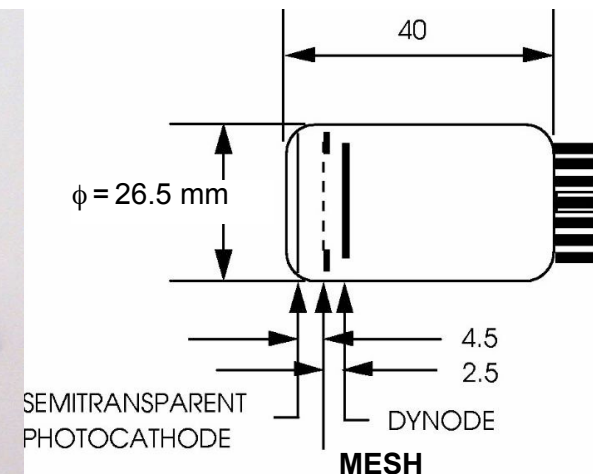
APD: ECAL barrel

Photo-electrons from THIN $6\mu\text{m}$ p-layer induce avalanche in p-n junction
 Electrons from ionising particles traversing the bulk are NOT amplified

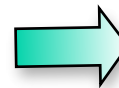
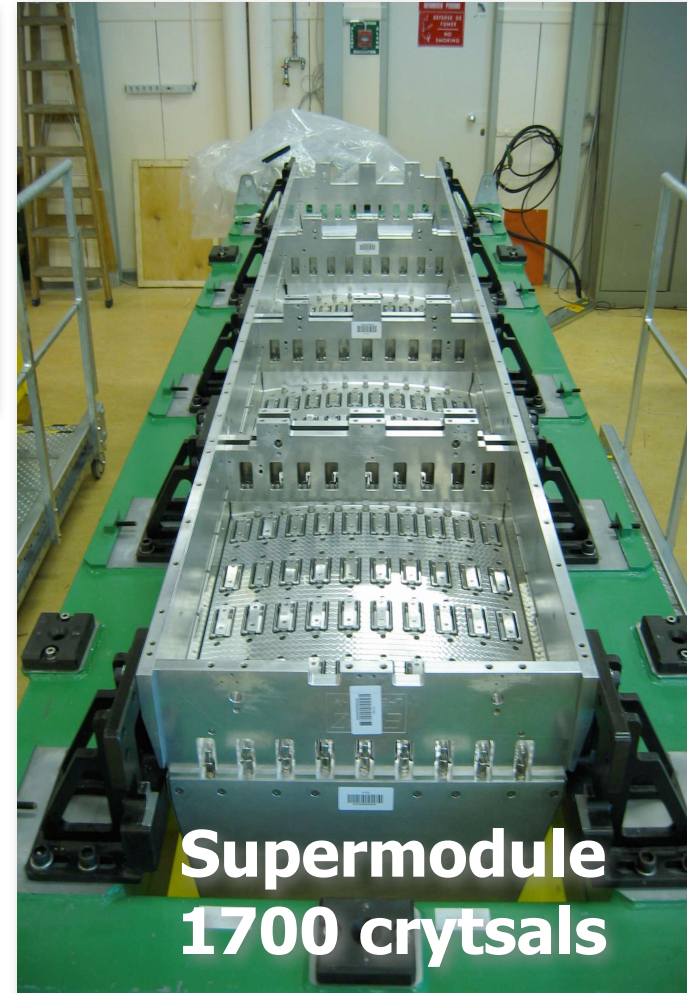
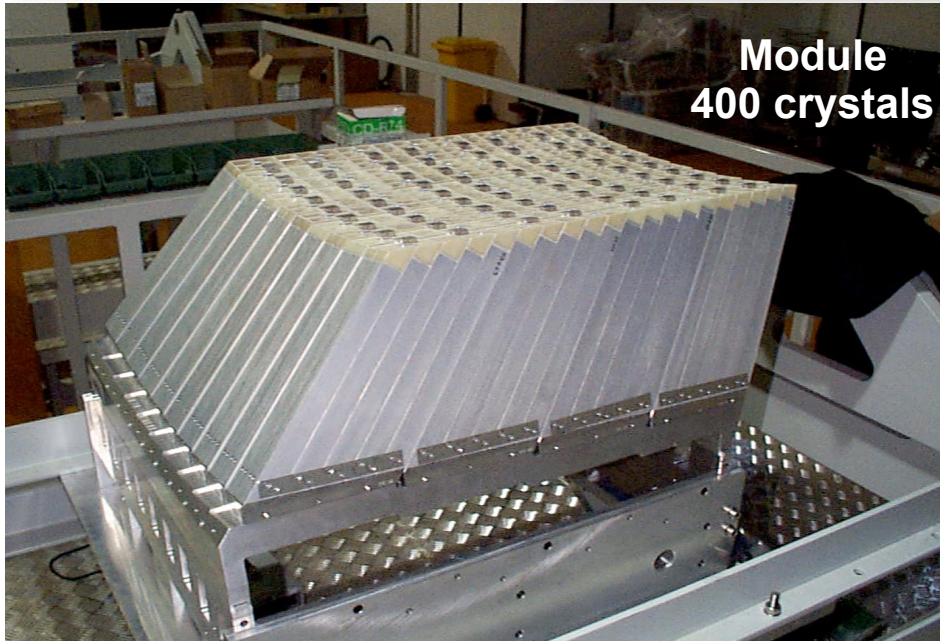
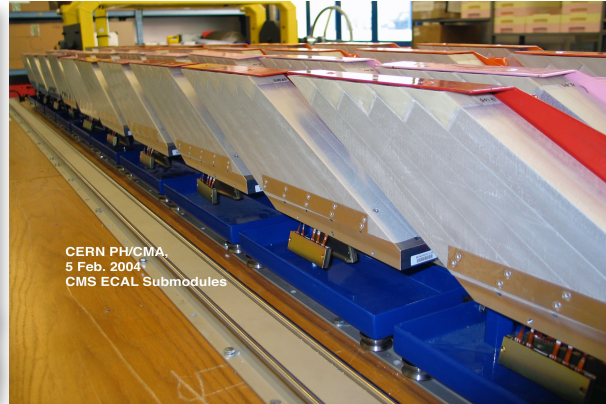
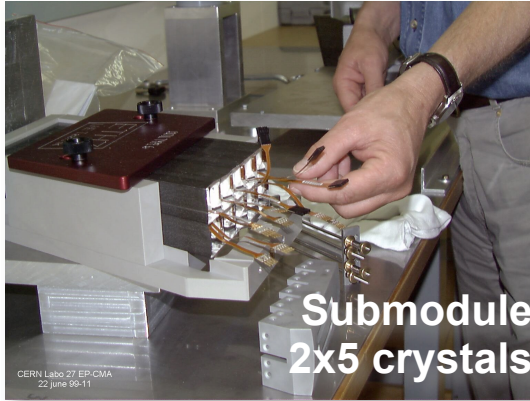


Vacuum Phototriodes: ECAL Endcaps

Single stage PM tube with fine metal grid anode (insensitive to axial magnetic fields)
 Favourable for EC-ECAL
 Q.E. $\sim 20\%$ at 420nm

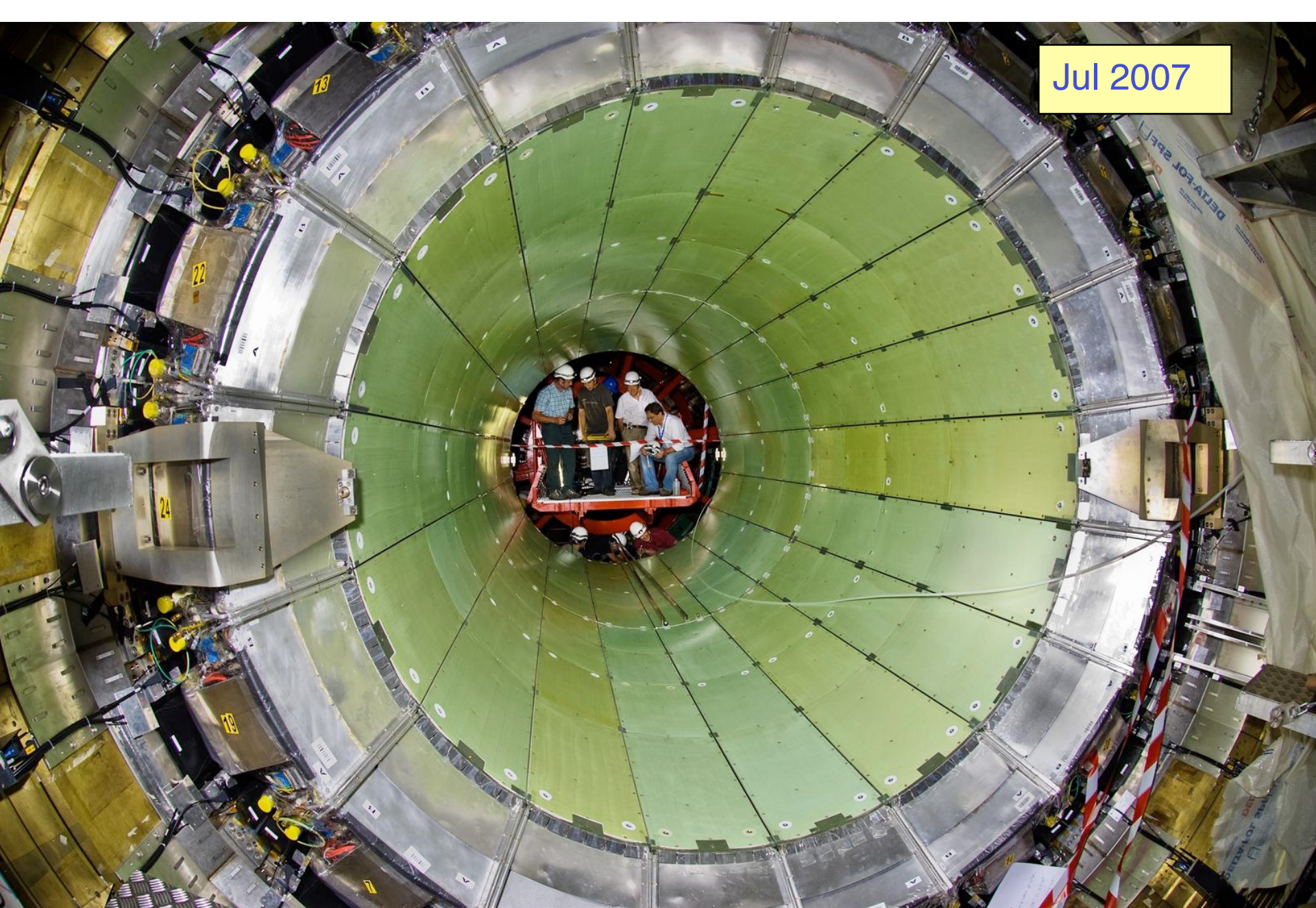


CMS ECAL Construction



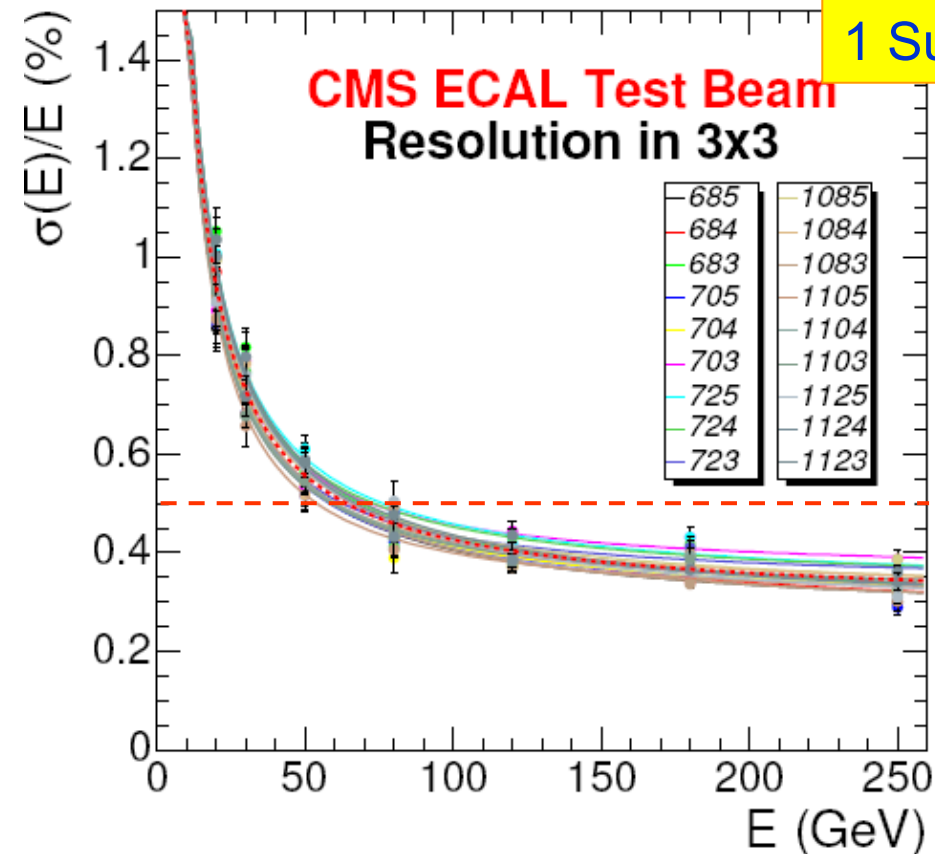
Total 36 Supermodules

Jul 2007



CMS ECAL: Performance in testbeam

1 Super Module 1700 xl on test beam in 2004



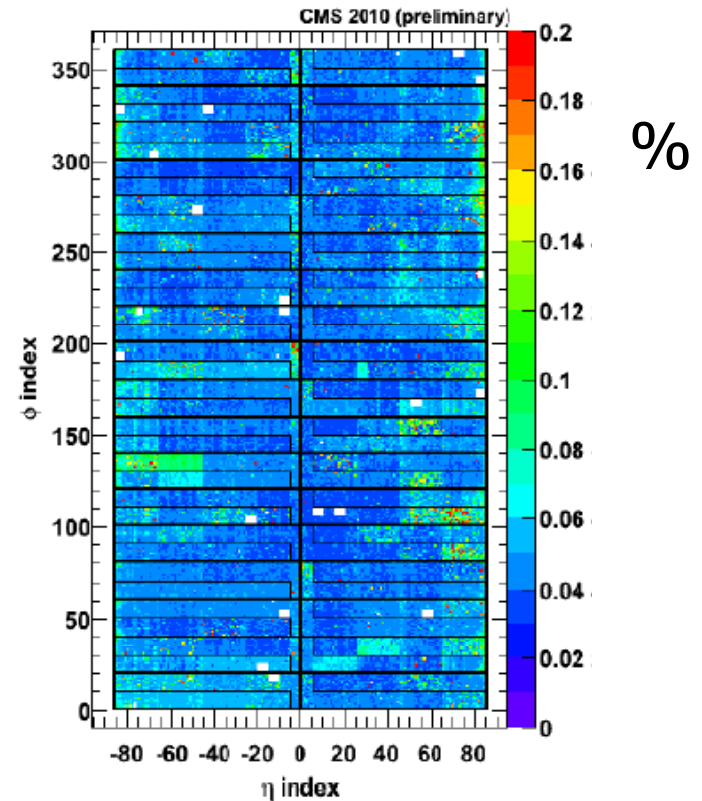
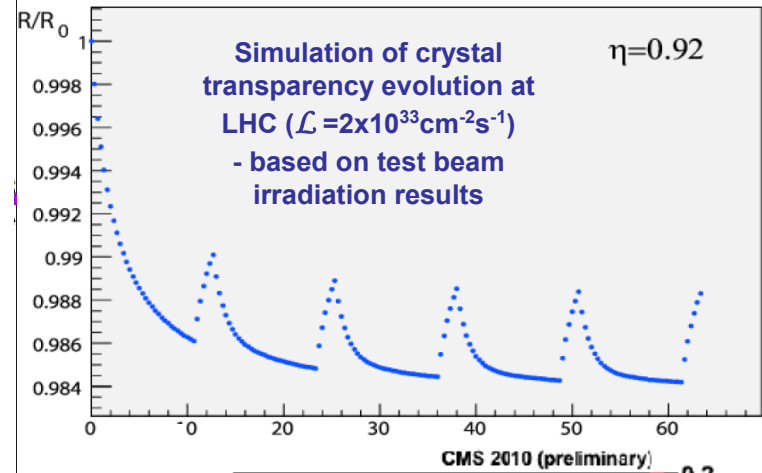
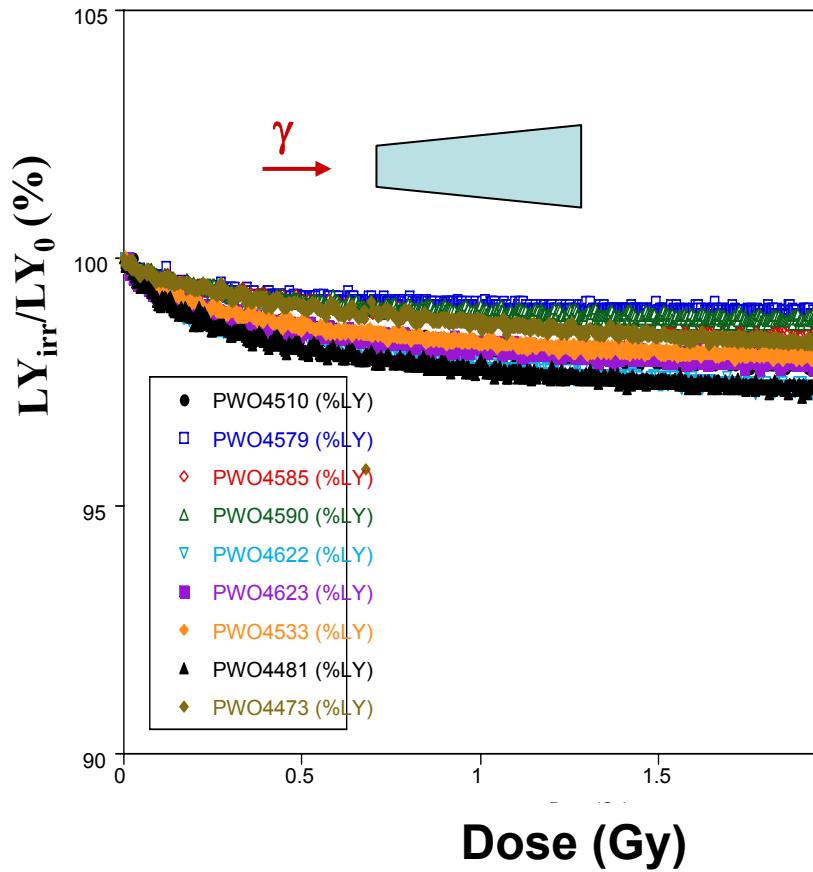
Excellent performance obtained in testbeam

1/4 of barrel modules

How to preserve it at LHC ?

$$\frac{\sigma}{E} = \frac{2.8\%}{\sqrt{E(\text{GeV})}} \oplus \frac{125}{E(\text{MeV})} \oplus 0.3\%$$

Sensitive to radiation dose



Large effect which needs to be corrected for

Laser system which sends light to each crystal during beam (LHC abort gap)

Crystal calibration in CMS

Inter-calibration: several steps

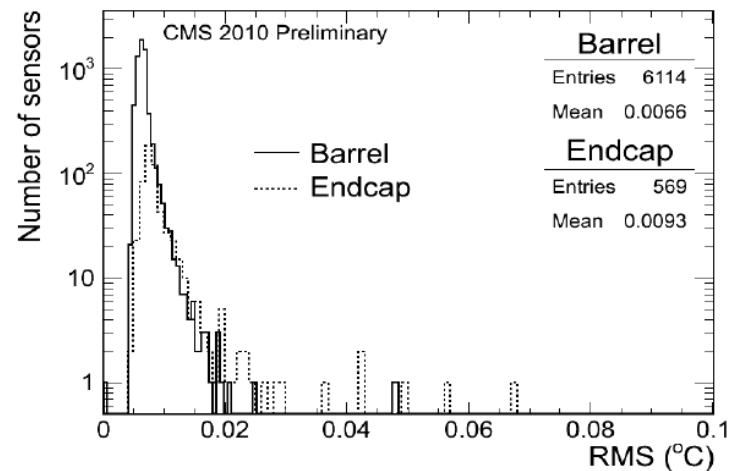
testbeam (1/4 of barrel ECAL)

cosmic muons in situ

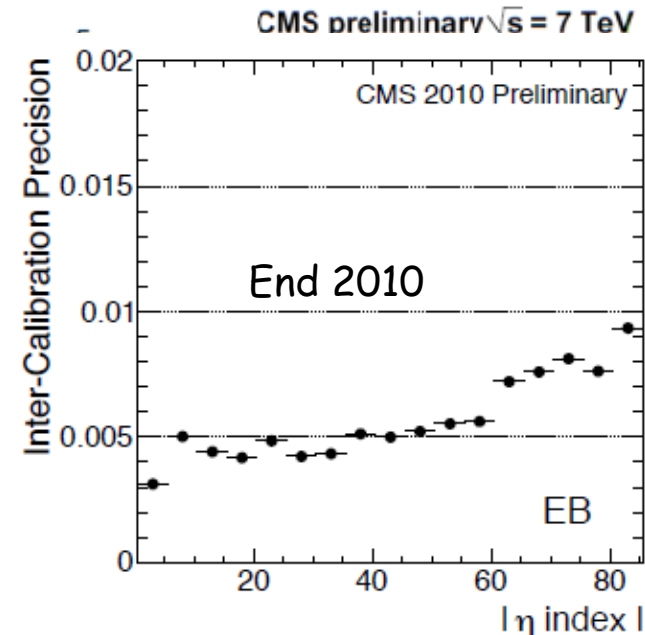
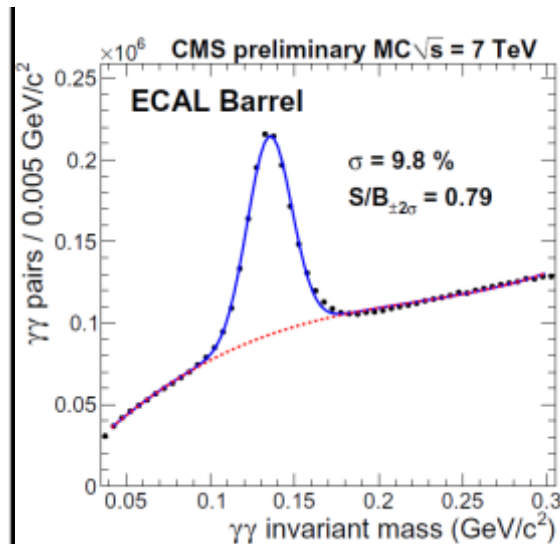
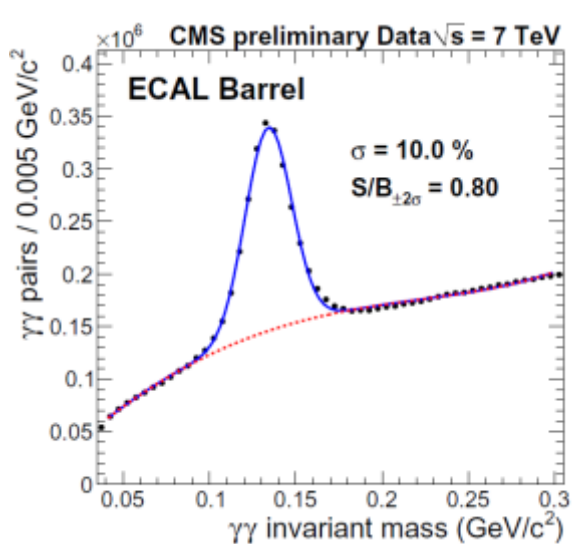
Laser pulsing: tracks variations during data taking

Temperature stability: $\Delta E/E = -2\%/^{\circ}\text{C}$

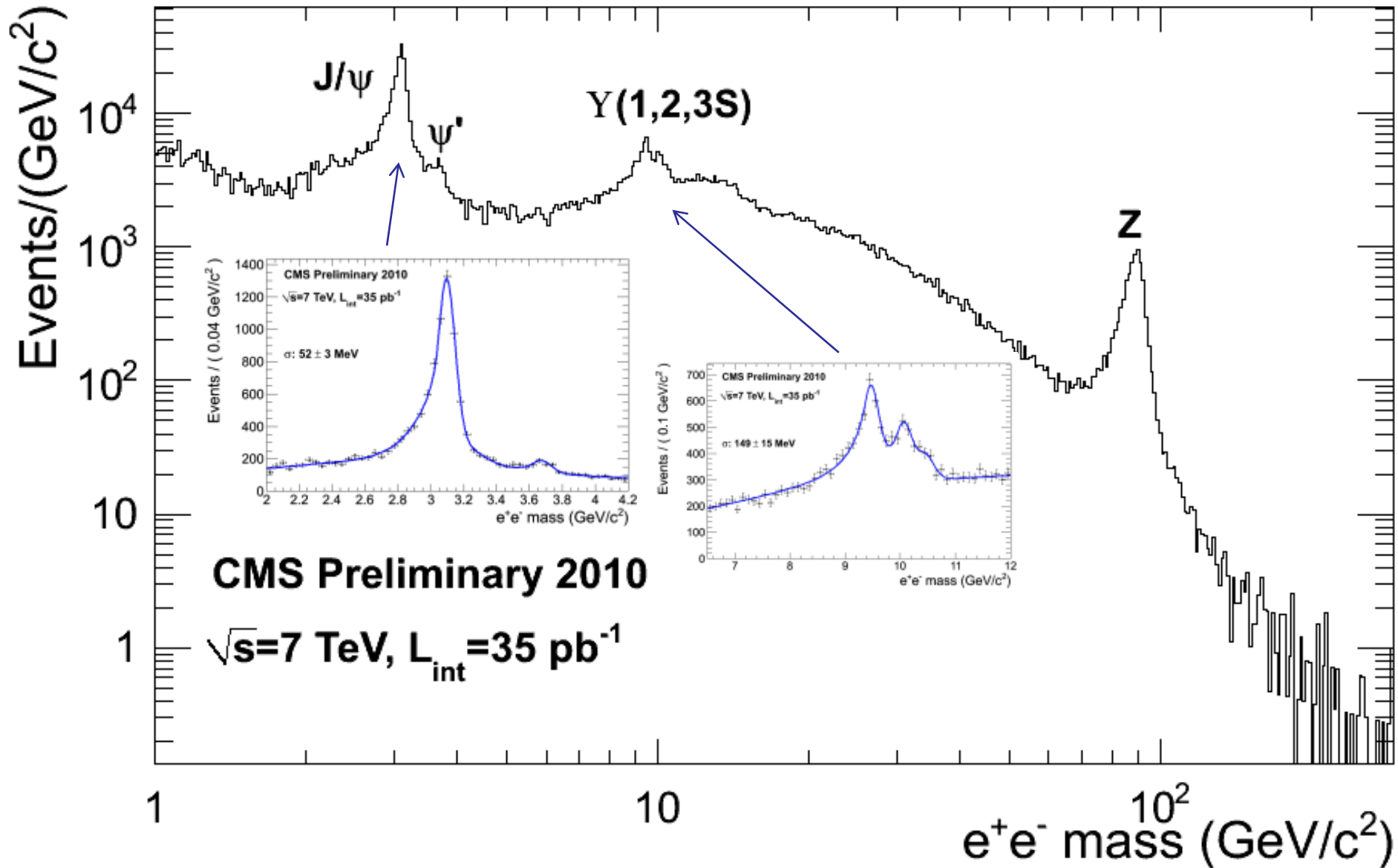
Using particles: π^0, η^0



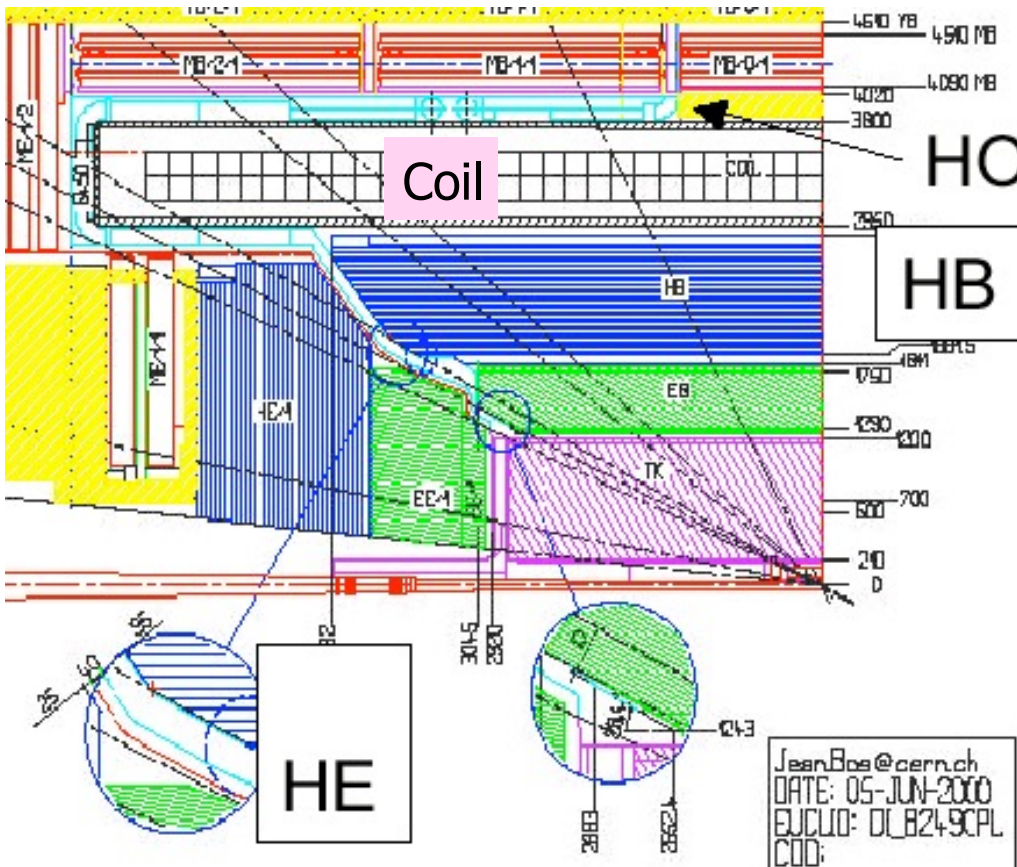
June 2010 - Dec 2010



Performance in-situ CMS



CMS Hadronic calorimeter



Central : $|\eta| < 1.7$ Cu/scintillator + WLS

2 + 1 (HO) layers

$5.9 + 3.9 \lambda$ ($|\eta| = 0$)

Endcap $1.3 < |\eta| < 3$ Cu/scintillator + WLS

2/3 layers

Forward $2.85 < |\eta| < 5.19$

Fe/quartz fibers (radiations)

Copper: non magnetic material

CMS Hadronic Response

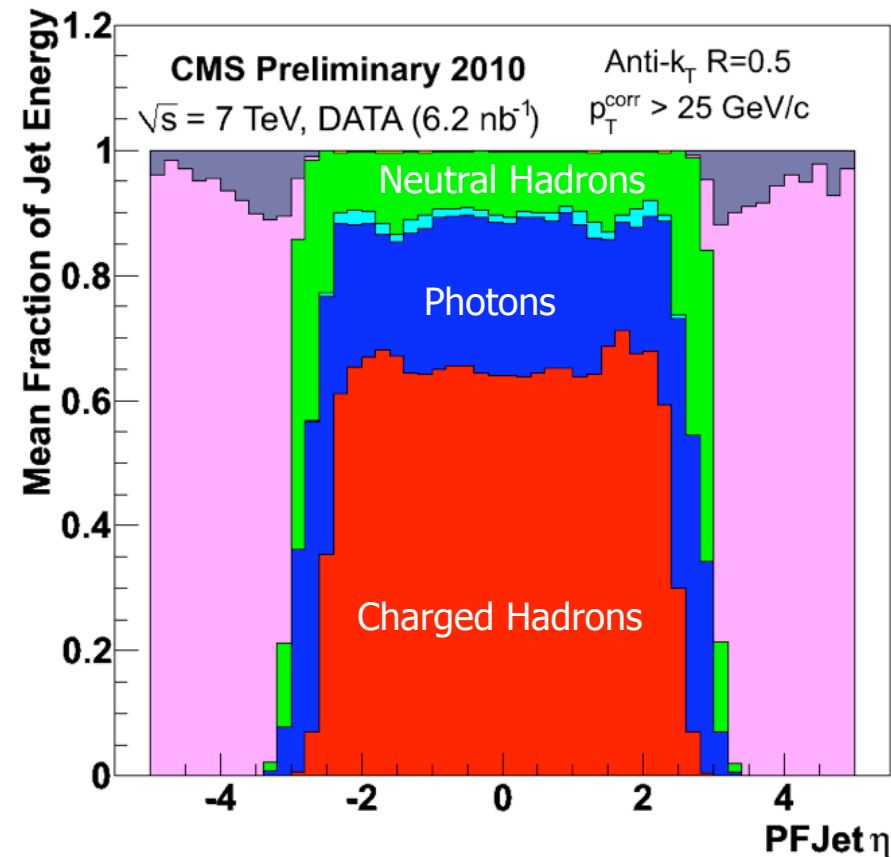
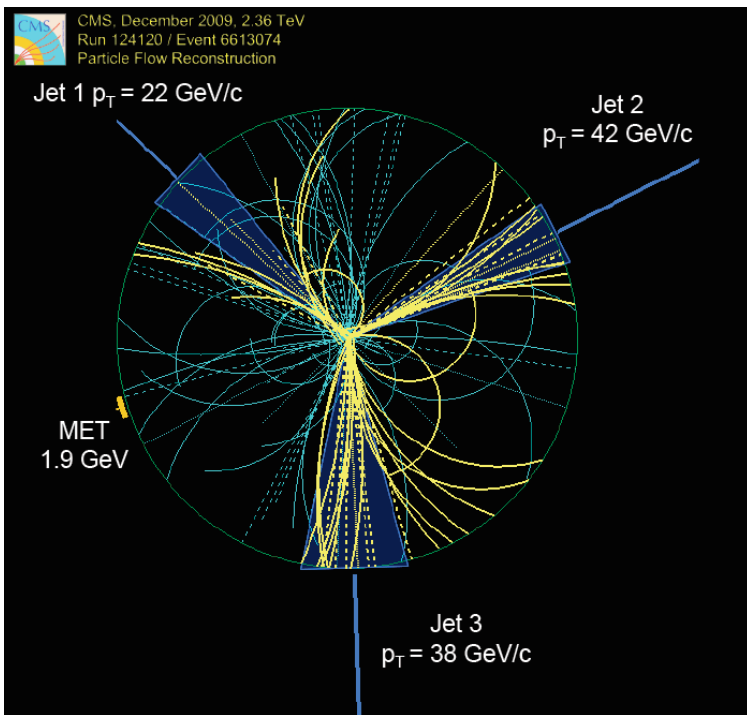
CMS is using a Particle Flow Technic to reconstruct Jets and Missing Transverse Energy

use the best measurement for each component

Tracker for charged hadron

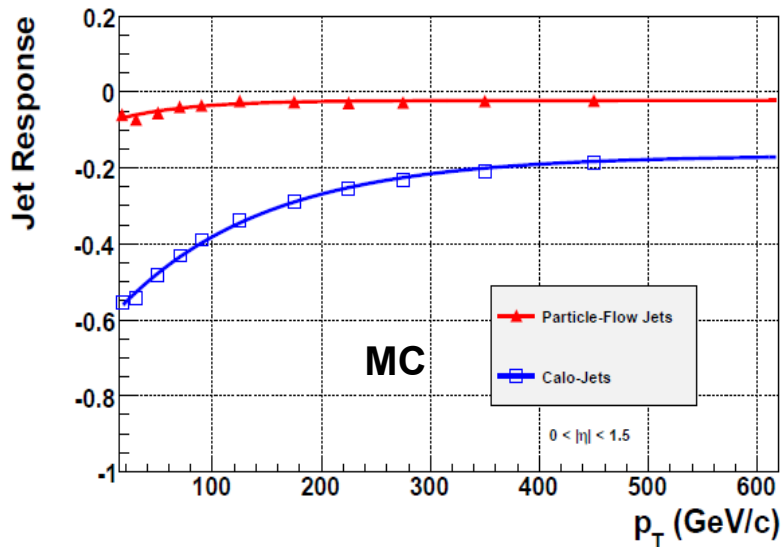
ECAL for electrons & photons

HCAL for neutral hadrons

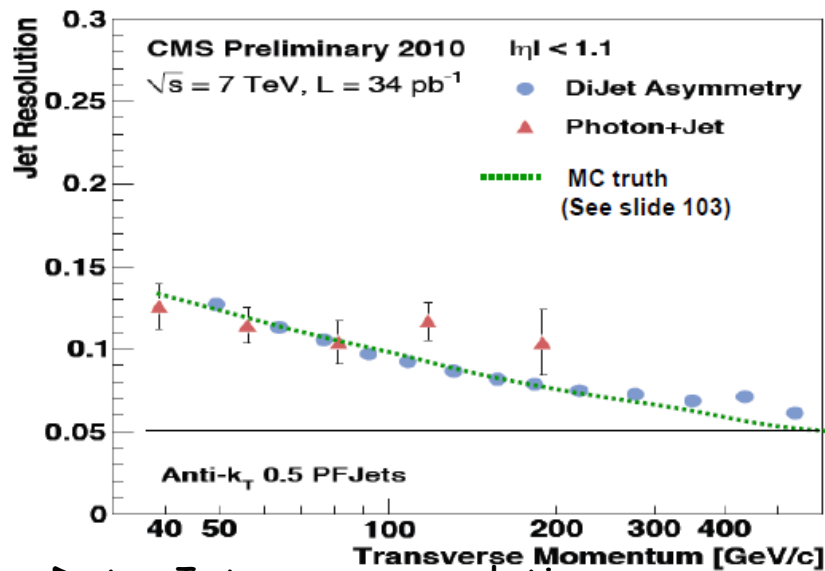
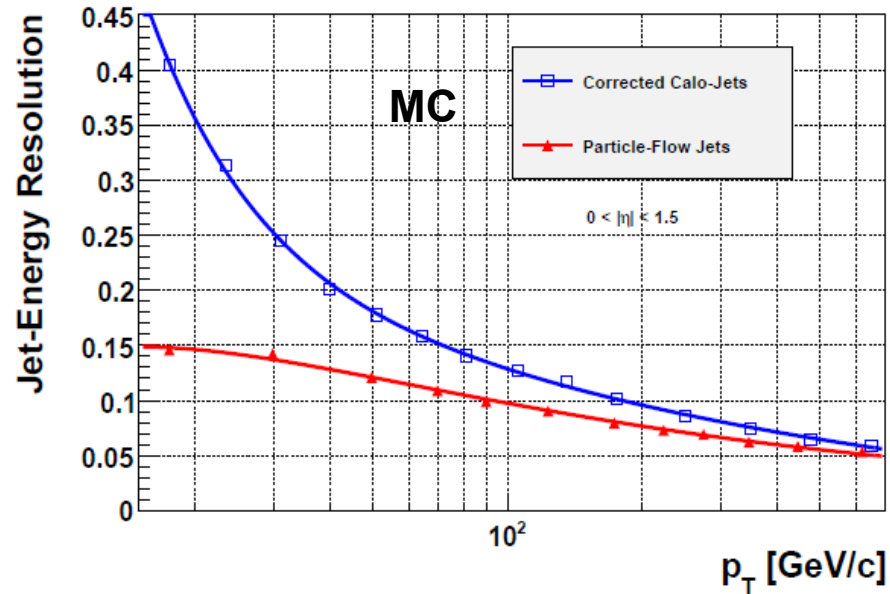


CMS-Particle Flow Jet Reconstruction Performance

CMS Preliminary



CMS Preliminary



ATLAS calorimeter

ATLAS EM calorimeter

Accordion Pb/LAr $|\eta| < 3.2$ $\sim 170k$ channels

Precision measurement $|\eta| < 2.5$

3 layers up to $|\eta| = 2.5$ + presampler $|\eta| < 1.8$

2 layers $2.5 < |\eta| < 3.2$

Layer 1 (γ/π^0 rej. + angular meas.)

$\Delta\eta \cdot \Delta\phi = 0.003 \times 0.1$

Layer 2 (shower max)

$\Delta\eta \cdot \Delta\phi = 0.025 \times 0.025$

Layer 3 (Hadronic leakage)

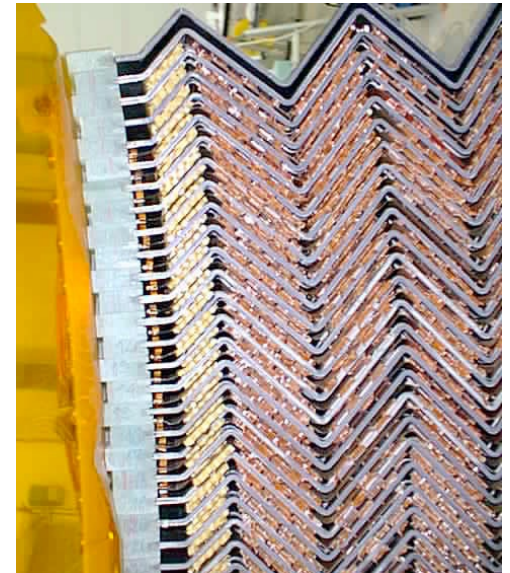
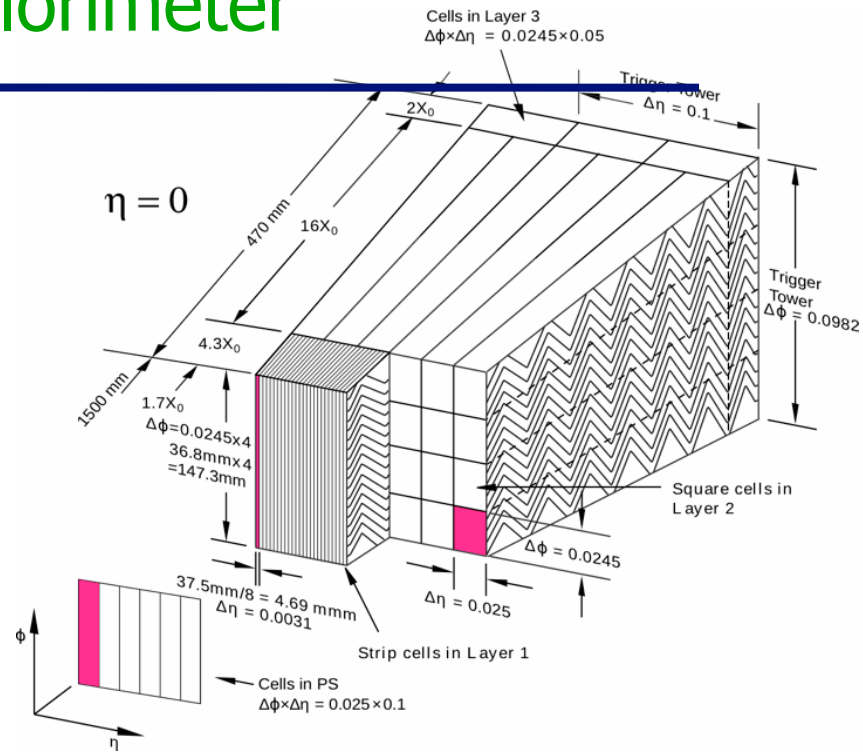
$\Delta\eta \cdot \Delta\phi = 0.05 \times 0.025$

Energy Resolution: design for $\eta \sim 0$

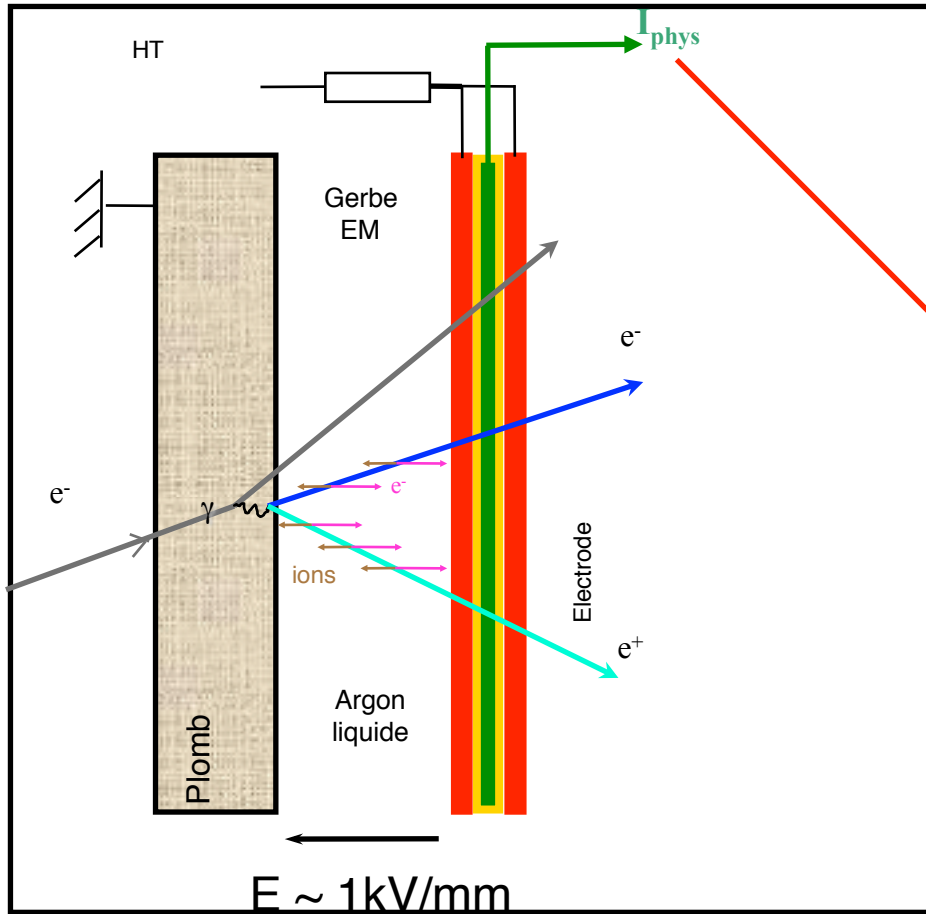
$\Delta E/E \sim 10\%/\sqrt{E} \oplus 150 \text{ MeV}/E \oplus 0.7\%$

Angular Resolution

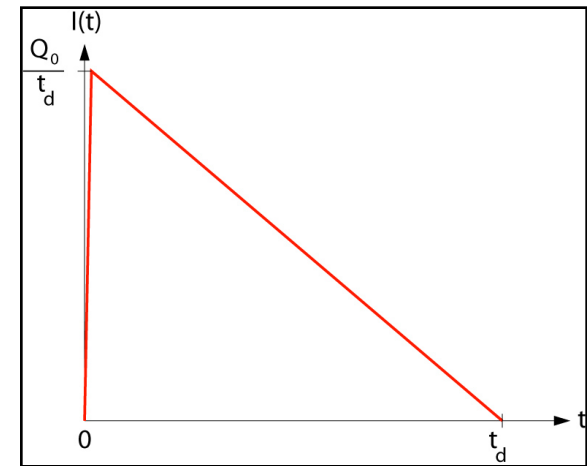
$50 \text{ mrad}/\sqrt{E(\text{GeV})}$



Principle



$\text{Pic} \propto \int \text{signal déposé}$

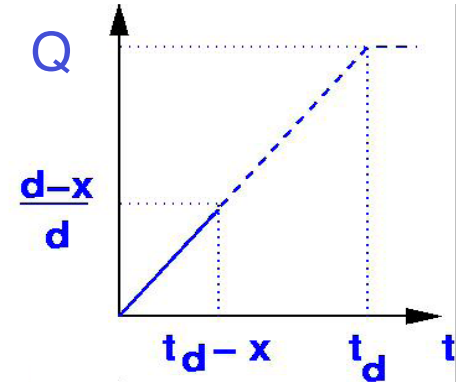
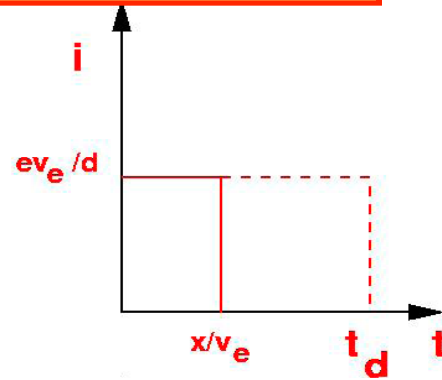
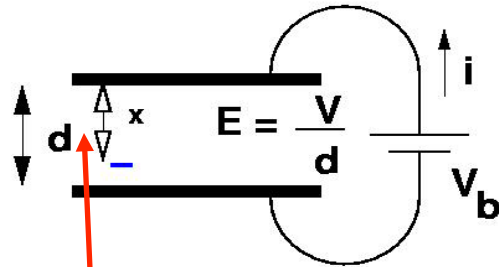


$400\text{ ns} \approx 16\text{ LHC BC}$

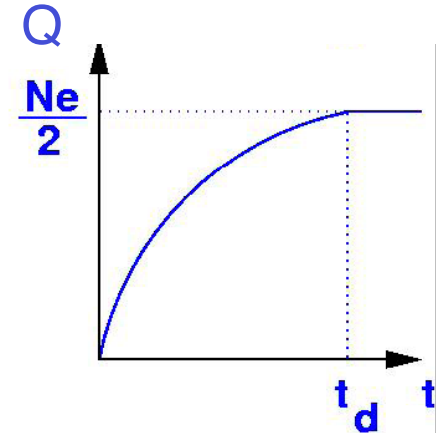
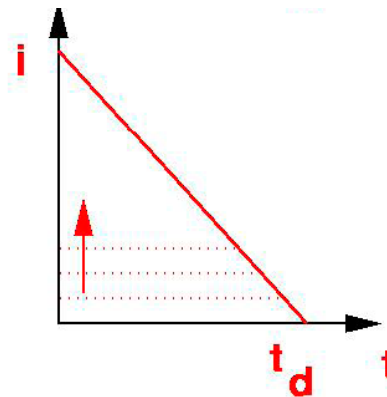
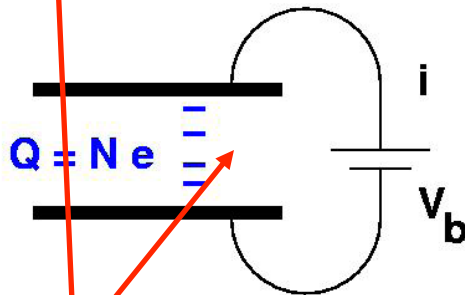
Collection du signal dans l'argon liquide

Collection des électrons induits par l'ionisation des atomes due au passage des particules chargées de la gerbe dans le liquide noble

Une charge



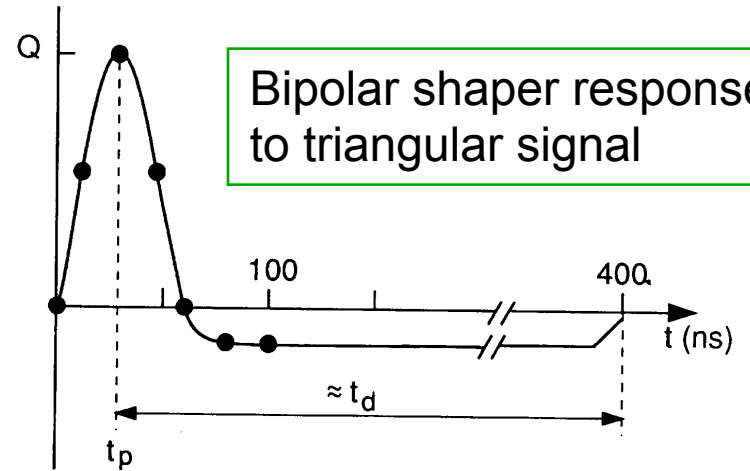
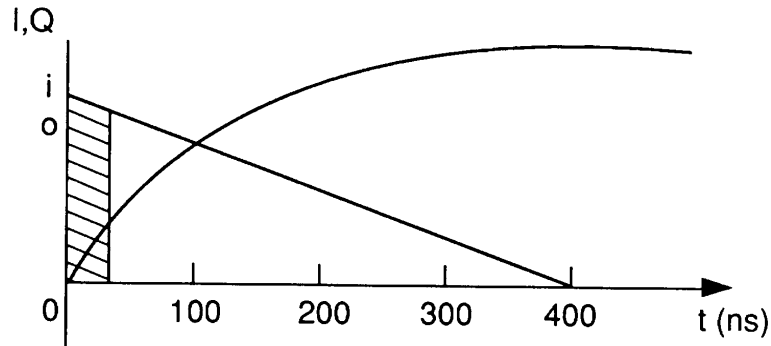
N charges uniformément réparties



Le gap

Obtaining a fast response

Integrate the current over time $t_p \ll t_D$ ($t_p \sim 40$ ns)



Bipolar shaper response to triangular signal

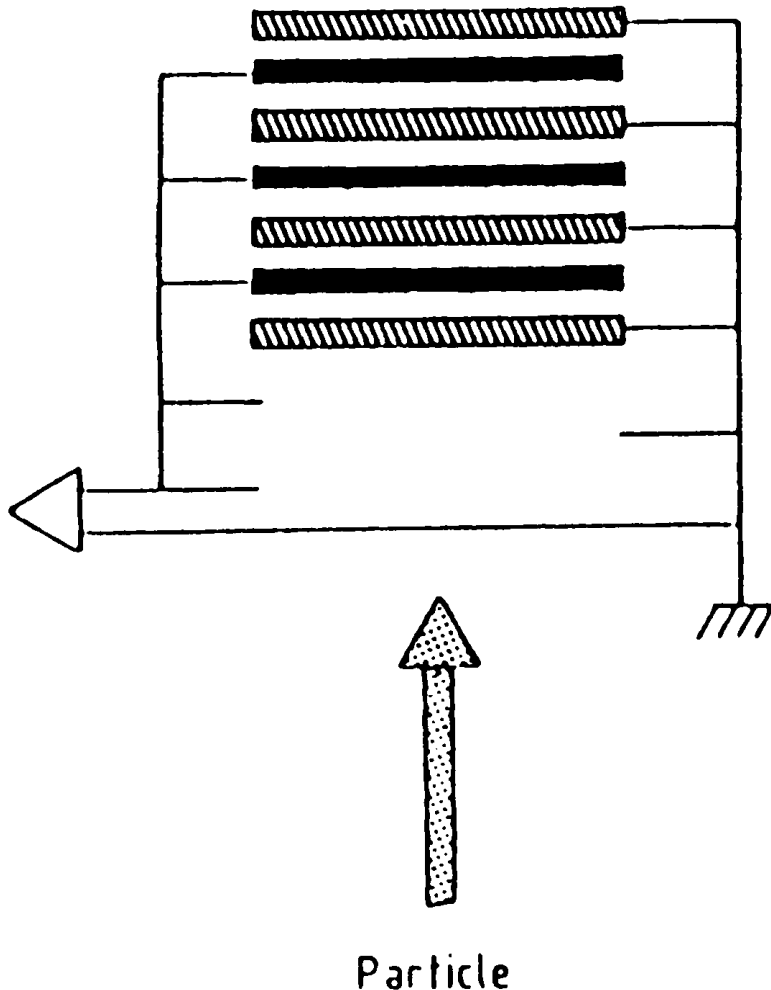
S/N is smaller than in the case $t_p = t_D$

$$S \sim t_p, N \sim \frac{1}{\sqrt{t_p}} \Rightarrow \frac{S}{N} \sim t_p^{3/2}$$

→ detector response time is not t_d but t_p

~30 smaller for 40 ns than for 400 ns

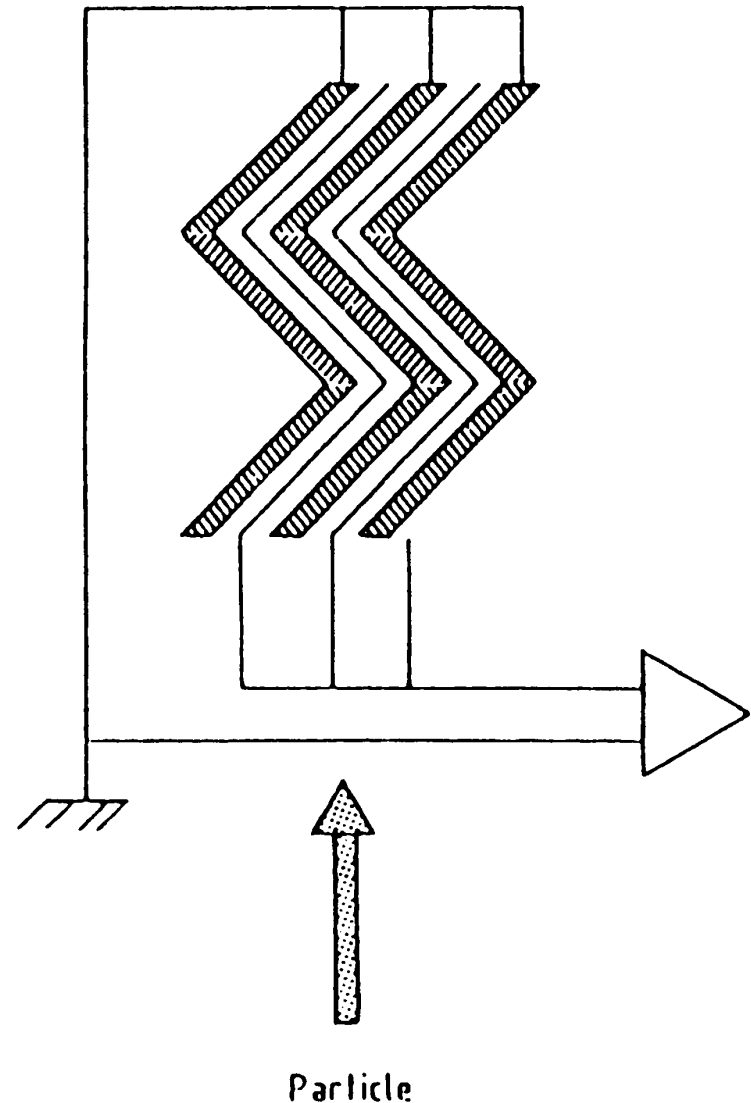
Parallel plates geometry



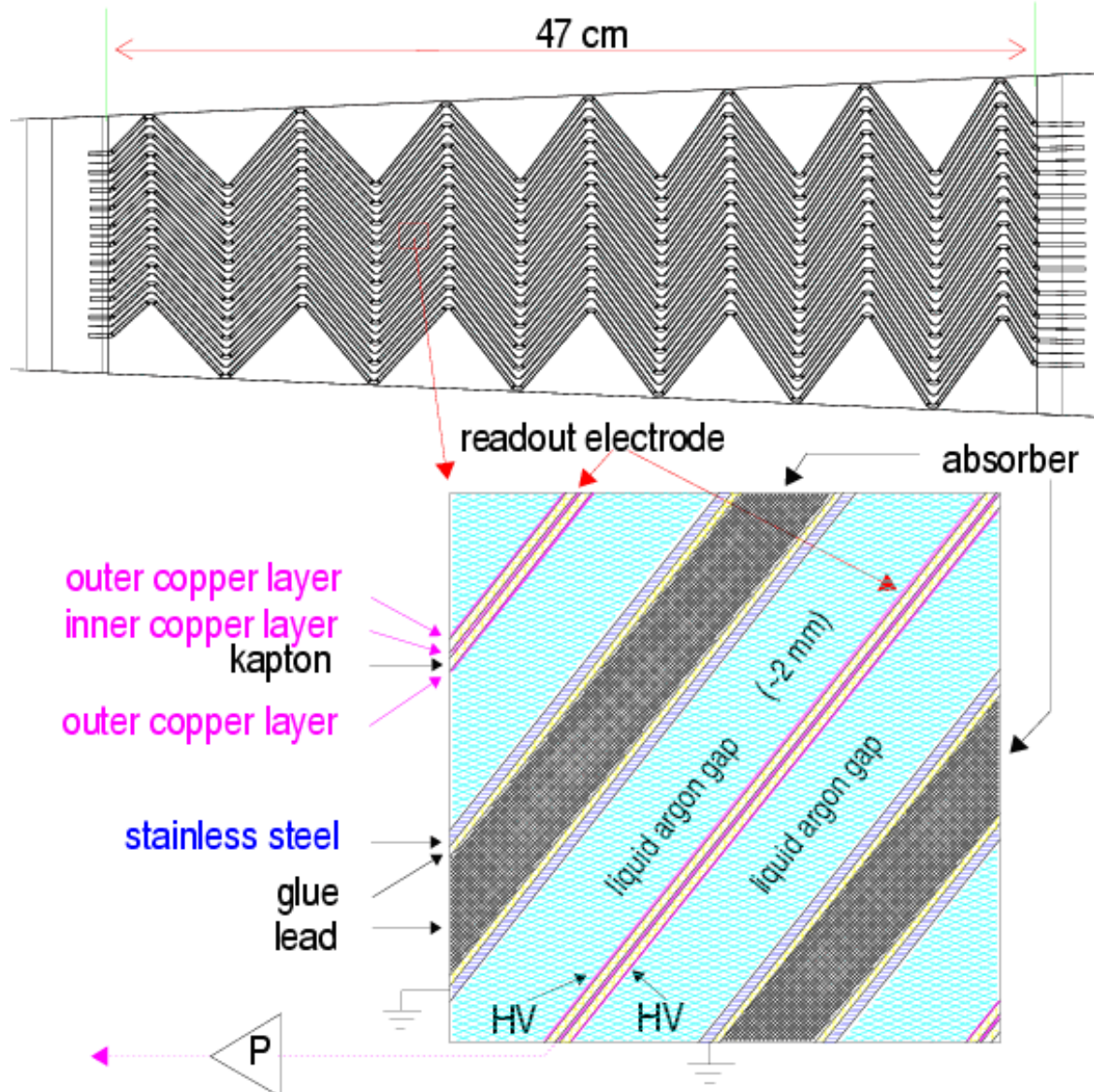
- Les anciens calorimètres à argon liquide avaient un temps de réponse lent (intégration du signal).
- Electrodes perpendiculaires aux particules
- Longs câbles
pour emmener les signaux vers les preamplis (transfert \sim qques ns)
regrouper ensemble des gaps
- Zones mortes dues aux câbles

Accordeon geometry

- Géométrie à accordéon:
rapide
- Les électrodes sont parallèles aux particules incidentes
 - lectures des signaux à l'avant et à l'arrière
 - pas de longues connexions
- Le découpage en profondeur est dessiné sur les électrodes
- **Pas d'espace sans détection**

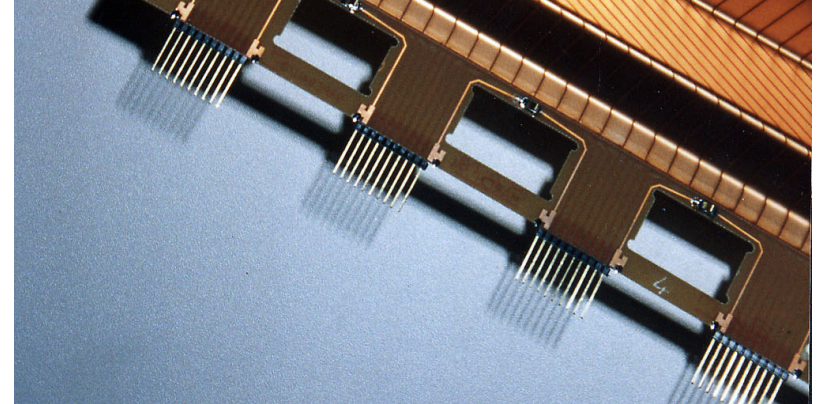
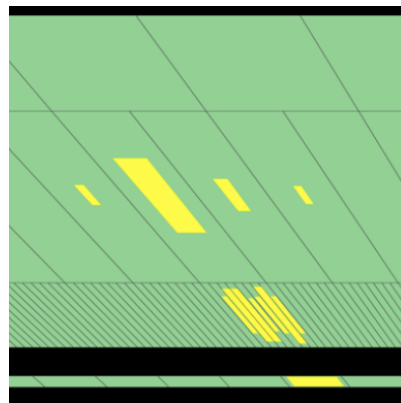
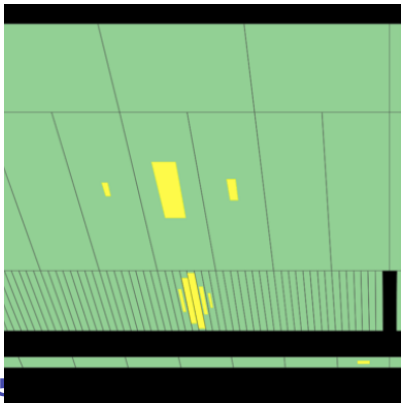
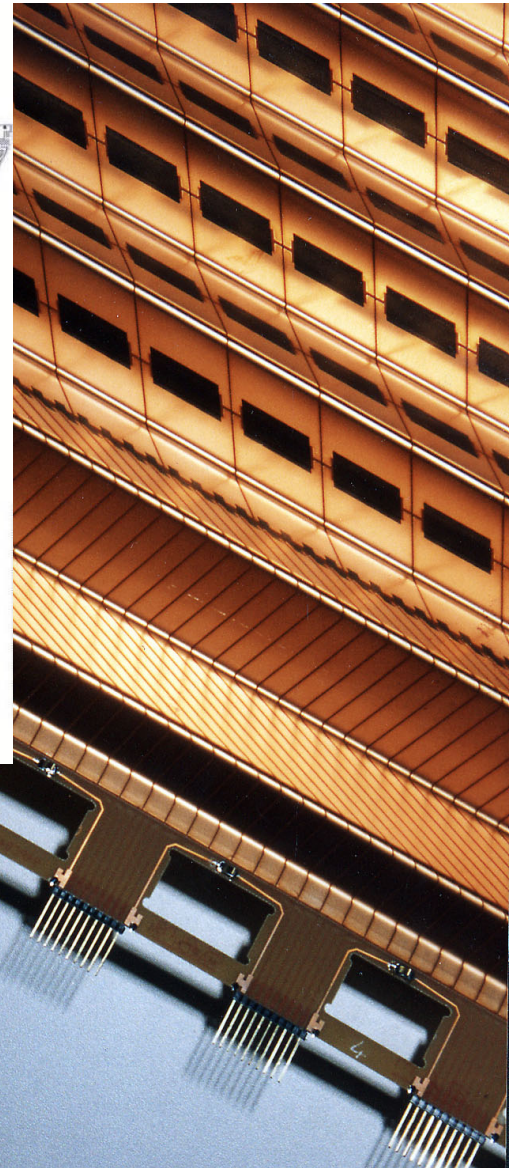
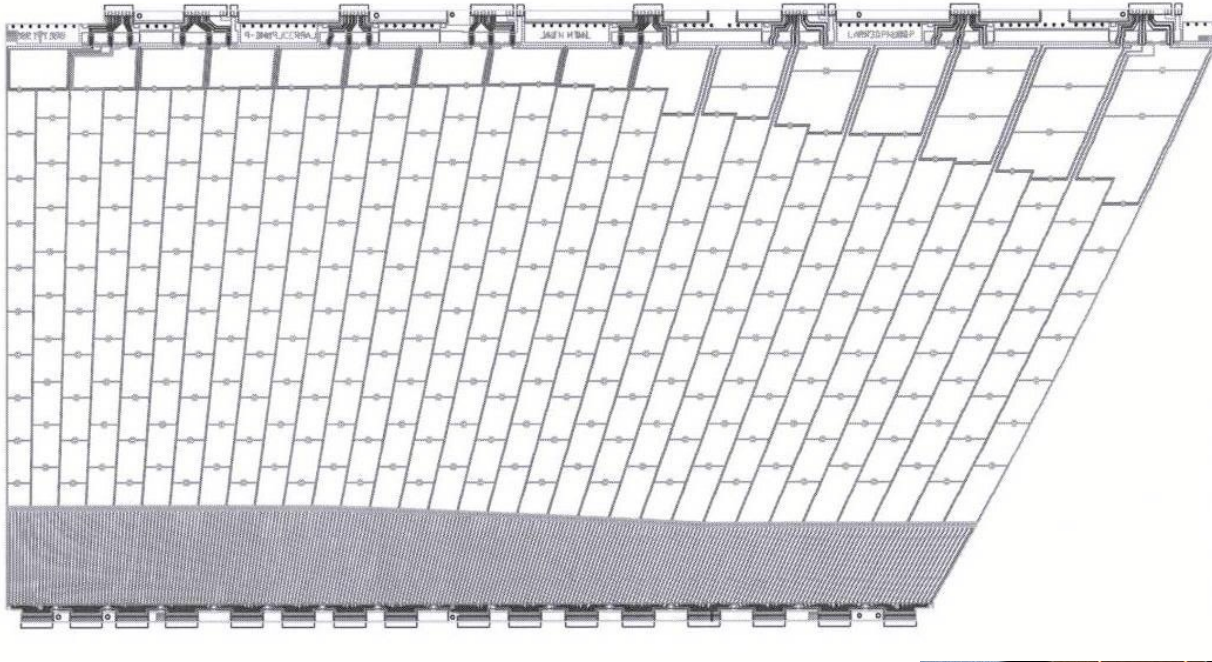


ATLAS EM calorimeter

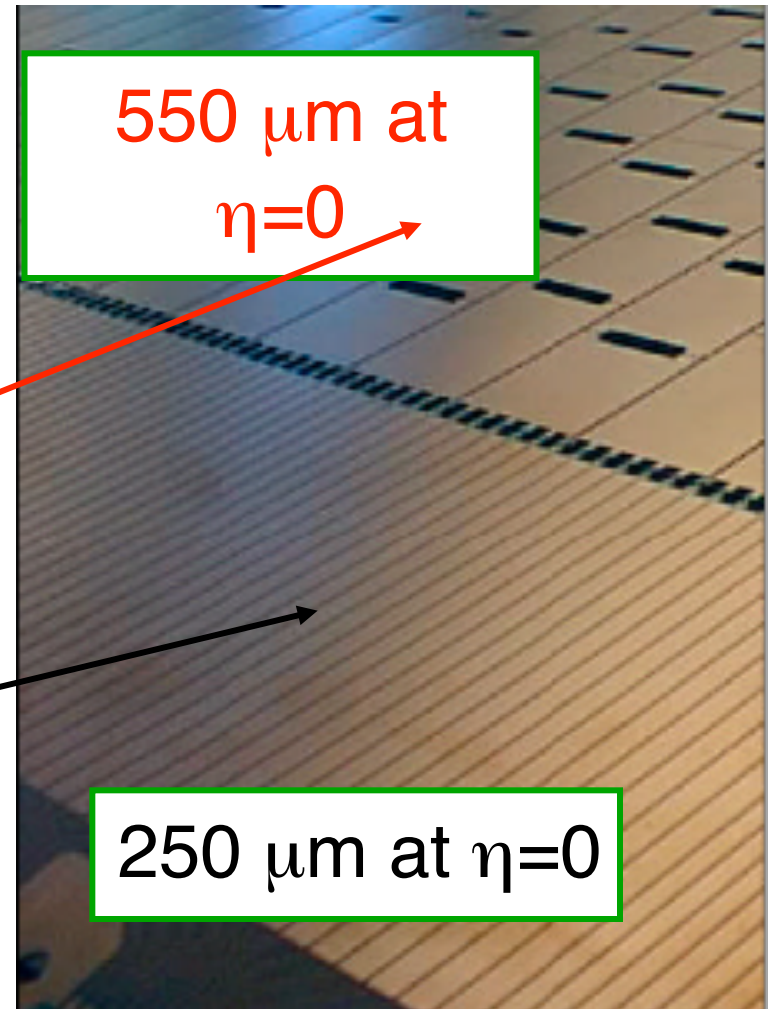
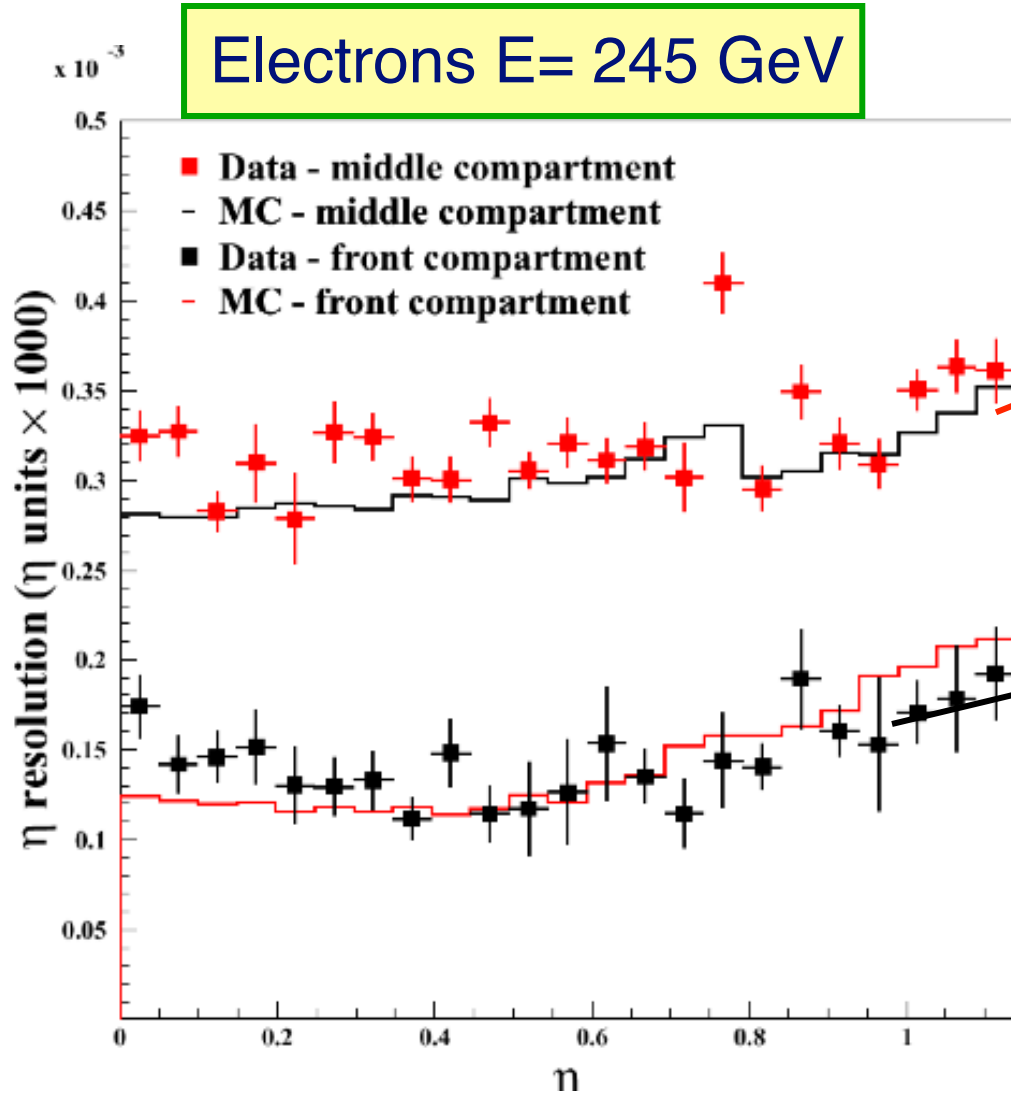


The segmentation

origine27.dwg du 02/07/1999



Position resolution



Energy Resolution CMS vs ATLAS

| CMS (PbWO ₄) / ATLAS (Pb/LAr) | | | |
|---|--------------|-------------|-------------|
| | 10 GeV | 100 GeV | 1000 GeV |
| Stochastic (GeV) | 0.095 / 0.32 | 0.3 / 1 | 0.949 / 3.2 |
| Noise (GeV) | 0.3 / 0.3 | 0.3 / 0.3 | 0.3 / 0.3 |
| Constant (GeV) | 0.05 / 0.07 | 0.5 / 0.7 | 5 / 7 |
| $\sigma(E)$ (GeV) | 0.30 / 0.44 | 0.65 / 1.26 | 5.1 / 7.7 |
| $\sigma(E)/E$ (%) | 3 / 4.4 | 0.65 / 1.26 | 0.51 / 0.77 |

$$\frac{\sigma(E)}{E} = \frac{0.03}{\sqrt{E(\text{GeV})}} \oplus \frac{0.3}{E(\text{GeV})} \oplus 0.005$$

$$\frac{\sigma(E)}{E} = \frac{0.1}{\sqrt{E(\text{GeV})}} \oplus \frac{0.3}{E(\text{GeV})} \oplus 0.007$$